Published in Cretaceous Research 29, issues 5-6, 976-994, 2008
which should be used for any reference to this work

Oceanic events and biotic effects of the Cenomanian-Turonian anoxic event, Tarfaya Basin, Morocco

G. Keller [a,*], T. Adatte [b], Z. Berner [c], E.H. Chellai [d], D. Stueben [c]

[a] *Department of Geosciences, Princeton University, Princeton NJ 08540, USA*
[b] *Geological Institute, University of Neuchatel, Neuchatel, CH-2007, Switzerland*
[c] *Institute for Mineralogy & Geochemistry, University of Karlsruhe, 76128 Karlsruhe, Germany*
[d] *University Cadi Ayyad, Faculty of Sciences Semlalia, Marrakech, Morocco*

A B S T R A C T

Profound biotic changes accompanied the late Cenomanian $\delta^{13}C$ excursion and OAE2 in planktic foraminifera in the Tarfaya Basin of Morocco. Planktic foraminifera experienced a severe turnover though no mass extinction, beginning with the rapid $\delta^{13}C$ excursion and accelerating with the influx of oxic bottom waters during the first peak and trough of the excursion. Species extinctions equaled the number of evolving species, though only the disaster opportunists *Guembelitria* and *Hedbergella* thrived along with a low oxygen tolerant benthic assemblage. The succeeding $\delta^{13}C$ plateau and organic-rich black shale deposition marks the anoxic event and maximum biotic stress accompanied by a prolonged drop in diversity to just two species, the dominant (80–90%) low oxygen tolerant *Heterohelix moremani* and surface dweller *Hedbergella planispira*. After the anoxic event other species returned, but remained rare and sporadically present well into the lower Turonian, whereas *Heterohelix moremani* remained the single dominant species. The OAE2 biotic turnover suggests that the stress to calcareous plankton was related to changes in the watermass stratification, intensity of upwelling, nutrient flux and oxic levels in the water column driven by changes in climate and oceanic circulation. Results presented here demonstrate a 4-stage pattern of biotic response to the onset, duration, and recovery of OAE2 that is observed widely across the Tethys and its bordering epicontinental seas.

Keywords: Cenomanian-Turonian, Biotic effects, Oceanic events, Tarfaya, Morocco

1. Introduction

The middle through early Late Cretaceous (~120–80 Ma) was a time of extreme warming commonly attributed to high levels of atmospheric greenhouse gases and high sea levels repeatedly drowning reefs and creating large shallow continental seas. Distinct intervals of black shale deposition with unusually high concentrations of total organic carbon (TOC) termed oceanic anoxic events (OAE) were deposited on a global scale during the Aptian-Albian, Cenomanian-Turonian and Coniacian-Santonian (e.g., Hart and Leary, 1989; Crowley, 1991; Johnson et al., 1996; Wilson et al., l998; Jones and Jenkyns, 2001; Norris et al., 2002; Leckie et al., 2002). At these times, the sequestration of the organic carbon due to high burial rates favored the formation of petroleum source rocks and reduced atmospheric PCO_2, which affected climate (e.g., Kuypers et al., 1999; Kolonic et al., 2005). OAEs are commonly attributed to the formation of large igneous provinces (LIPs) and associated hydrothermal activity (Larson and Erba, 1999), enhanced upwelling and nutrient cycling driven by orbital forcing (Wagner et al., 2004; Kuhnt et al., 2004; Kolonic et al., 2005).

An intense and widespread period of oceanic anoxia and high TOC accumulation in black shales occurred during the late Cenomanian to early Turonian (known as OAE2). Extremely warm tropical oceans with sea surface temperatures 4–7 °C above modern mean annual temperatures are suggested to have intensified atmospheric energy transport and oceanic circulation leading to increased nutrient flux (Föllmi et al., 1994; Norris et al., 2002; Kuhnt et al., 2004). At the same time sea levels reached their Phanerozoic maximum (Haq et al., 1987; Hallam, 1992) accompanied by exceptionally high organic carbon burial in outer shelf and ocean basins associated with a global positive $\delta^{13}C$ excursion (Schlanger et al., 1987; Jarvis et al., 1988; Jenkyns et al., 1994; Gale et al., 1993; Accarie et al., 1996; Ulicny et al., 1997).

A major biotic turnover is associated with these environmental changes, though not the major mass extinction (i.e., 53% marine species extinct) as originally proposed based on invertebrate macrofossils (Raup and Sepkoski, 1982; Sepkoski, 1989; Jablonski, 1981). More recent studies on macrofossils reveal a pattern of immigration-emigration associated with sea level changes, rather than true extinctions (Harries, 1993; Gale et al., 2000), placing in

* Corresponding author.
E-mail address: gkeller@princeton.edu (G. Keller).

doubt the original data compilation. Planktic foraminifera show relatively minor species extinctions over time (Jarvis et al., 1988; Hart and Leary, 1989, 1991; Banerjee and Boyajian, l996; Hart, l996). High-resolution studies at Pueblo and Eastbourne indicate about 30% species extinct and an equal gain in evolutionary diversification (Keller et al., 2001; Keller and Pardo, 2004a). Calcareous nannofossils reveal only minor extinctions coupled with evolutionary diversification and species abundance changes (Lamolda et al., l994; Erba and Tremolada, 2004).

Popular scenarios link the biotic changes to a variety of factors, including the sea level transgression, changes in water-mass stratification, upwelling of nutrient-rich, oxygen depleted deep waters, enhanced productivity, expansion of the oxygen minimum zone (OMZ), deep water connection between the South and North Atlantic basins, and periodic photic zone and bottom water euxinia (e.g., Hart and Bigg, 1981; Jarvis et al., 1988; Hart and Ball, 1986; Hart, 1996; Paul et al., 1999; Gale et al., 2000; Leckie et al., 2002; Gebhardt et al., 2004; Keller et al., 2001, 2004; Wagner et al., 2004; Caron et al., 2006). However, the precise nature of events linking the faunal turnover to ongoing environmental changes remains unclear. This is partly because relatively few C-T sequences exist to date that provide the linked high-resolution quantitative faunal and geochemical records necessary to evaluate the precise timing, nature and extent of the faunal turnover across latitudes in continental shelf and open ocean environments and link these to the oceanic events. Many C-T outcrops are limited in terms of carbon and/or organic matter preservation and hence provide incomplete faunal and geochemical records.

The most complete sequences and best-studied localities to date are in the US Western Interior (Pueblo stratotype), UK (Eastbourne) and the Tarfaya basin of southern Morocco. Each of these localities exhibits rhythmic sedimentation indicating orbital scale forcing and permitting millennial-scale time resolution (Gale et al., 2002; Meyers et al., 2001, 2005; Kolonic et al., 2005; Kuhnt et al., 1997, 2004; Sageman et al., 2006). Among these three localities, the Tarfaya C-T sequences exposed along the Atlantic coast of south-western Morocco accumulated exceptionally high rates of black shale (up to 12 cm/ky, Kuhnt et al., 1997, 2004) and burying an estimated ~2% of the overall global excess of organic carbon associated with the OAE2 (Kolonic et al., 2005).

We investigated four outcrops in the Tarfaya Basin (Shell Quarry, Tazra, Amma Fatma, and Mohamed Beach, Fig. 1) and found only one (Tazra) with preservation suitable for quantitative planktic foraminiferal analysis. The results provide insights into the environmental conditions of the Cenomanian-Turonian anoxic event off northwestern Africa. The main objectives of this study include: (1) the evaluation of the biotic turnover and species extinctions in planktic foraminifera; (2) evaluation of the synchroneity of biotic and environmental events with respect to sections at Eastbourne, England, and the Pueblo, Colorado, global stratotype and point (GSSP); and (3) elucidate the relationship between biotic events, the $\delta^{13}C$ shift and ocean anoxia.

2. Geological setting and lithology

The Mesozoic Tarfaya Basin extends along the coast of southern Morocco between 28°N and 24°N (Fig. 1) and is part of the western margin of the Sahara platform, which has been tectonically stable since the Cretaceous (El Albani et al., 1999). Sediments consist of alternating layers of dark and light organic-rich shales and marly limestones that form the large-scale anticline structure of the Tarfaya Basin (Leine, 1986). During the late Cenomanian and early Turonian, deposition occurred in an open shelf setting to the south at a depth of 200–300 m (Kuhnt et al., 2001), but rapidly shallowed towards the paleoshoreline to the northeast, as indicated by increasing terrigenous influx (Tazra, Amma Fatma and Mohamed Beach, Gebhardt et al., 2004). In these shallower areas, sediments consist of dark-light laminated marly shales, marlstones and limestones with silicified nodules in some layers. The predominantly bioclastic limestone layers have erosive bases and hummocky cross-stratification. The carbonate is mainly biogenic consisting of foraminifera and calcareous nannofossils. Except for the Tazra section, organic carbon is generally well preserved as evident by the dark/light laminations prominently exposed along the cliffs of the Atlantic Ocean.

The Tazra section is located about 2 km inland from the Atlantic Ocean and exposed in a road cut about 30 km north of Tarfaya on the trans-Sahara highway from Tanger to Dakar (Fig. 2). About 10 m of upper Cenomanian to basal Turonian sediments are exposed below the road and facing the Tazra Sabkha, with about 6 m of the lower Turonian sequence continuing on the east side above the road. The outcrop shows strong surface weathering, which changed the black organic-rich sediments to a range of colors from yellow to brown to ochre reds, with the intensity of red color depending on the organic content (Fig. 2). Organic matter preservation is therefore generally poor. A marly limestone with common ammonite molds marks the base of the section (unit A, Fig. 3). Above it is

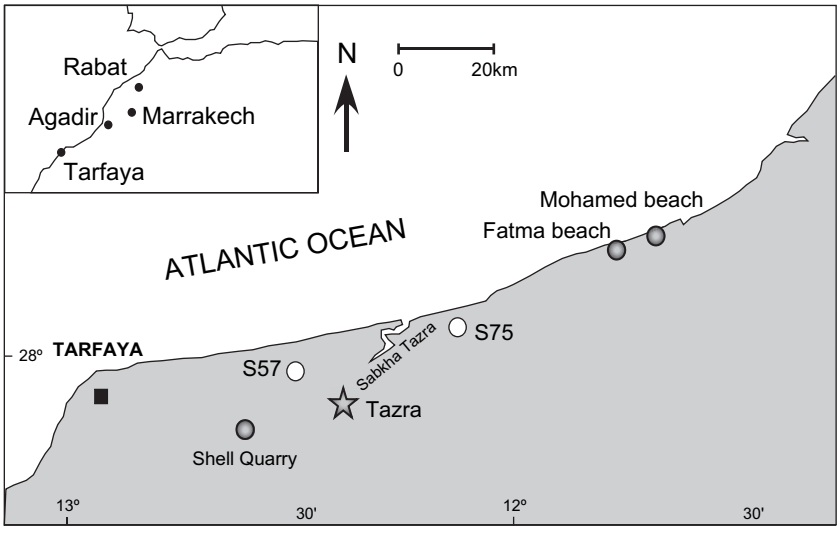

Fig. 1. Location of the Tarfaya Basin along the northwestern Atlantic margin of Morocco with outcrop and subsurface well localities (modified from Kuhnt et al.,2004).

Fig. 2. Exposure of the Tazra section just below the trans-Sahara highway from Tanger to Dakar, about 30 km north of Tarfaya.

a 2 m-thick laminated marly shale (unit B1), followed by 2 m of alternating marly limestones and laminated shale layers with ammonite molds (unit B2). Unit B3 consists of 1.5 m of laminated marly shale layers increasing in organic content upsection (intense red color). A 50 cm-thick limestone (unit C) underlies the 1.8 m-thick dark red laminated shale with siliceous nodules (unit D) and a thin limestone that characterizes the OAE2 at Tazra. Above it, marly limestones (unit E) and alternating limestone and shale layers (units F, G) mark the top of the section (Fig. 3).

3. Methods

The Tazra section was measured and examined for lithological changes, bioturbation and disconformities, and samples were collected at 10 to 20 cm intervals for microfossils, mineralogical and geochemical analyses. Ordinarily, strongly weathered outcrops, such as Tazra, are poor subjects for microfossil studies. However, in this case the removal of the organic-rich carbon made it easier to free foraminifera from the indurated bituminous and slightly silicified chalk. In the sections with well-preserved organic matter (e.g., Mohammed Beach, Amma Fatma) foraminifera are poorly preserved and difficult to free from adhering organic-rich carbon without dramatic use of ultrasound treatment, which may bias results due to breakage of smaller fragile specimens. However, other workers have succeeded in obtaining good foraminiferal records from subsurface cores using organic solvents and ultrasound treatments. In this study only the Tazra section was found to be suitable for quantitative faunal studies.

In the laboratory, processing for foraminifera followed standard procedure. The samples were crushed to pea-sized particles, placed in a beaker and immersed in dilute (3%) H2O2 for 1–2 days. The residues were then washed over a 63 μ screen, filtered and placed in the oven to dry at 50 °C. For faunal studies, the >63 μ size fraction was analyzed quantitatively for biostratigraphic and environmental analyses based on representative splits of 250–350 specimens per sample (Table 1). Species from each sample were picked, identified and mounted on microslides for a permanent record. Benthic foraminifera were counted to obtain a benthic/planktic ratio. The remaining sample residues were examined for rare species and these were entered in the species census and range data. The identification of species and classification of genera follows that of Eicher (1972), Robaszynski and Caron (1979), and Caron (1985).

For geochemical and mineralogical analyses, samples were dried, crushed, finely ground in an agate mill, and dried at 105°. Bulk rock analyses were conducted at the Geological Institute of the University of Neuchâtel, Switzerland, based on XRD analyses (SCINTAG XRD 2000 Diffractometre). Sample processing followed the procedure outlined by Kübler (1987) and Adatte et al. (1996). The origin and amount of organic matter were determined by Rock-Eval pyrolysis using a Rock-Eval 6 (Behar et al., 2001) at the Geological Institute of the University of Neuchâtel, Switzerland. Standard notations are used: TOC content in weight %; hydrogen index (HI = S2/TOC × 100) in mg hydrocarbons per g of TOC; oxygen index (OI = S3/TOC × 100) in mg CO2 per g of TOC.

Stable carbon and oxygen isotope analysis was performed on fine fraction bulk rock samples using a fully automated preparation system (MultiCarb) connected on-line to an "Optima" Isotope Ratio Mass Spectrometer at the University of Karlsruhe, Germany. All carbon and oxygen isotope values are reported relative to the PDB standard (Appendix Table 2). Precision of the reported values is better than ±0.05‰ and ±0.08‰ for $\delta^{13}C$ and $\delta^{18}O$, respectively (1 s definition). Accuracy was checked by repeated measurements of the NBS 19 carbonate standard. The average of 22 individual measurements was found to be identical with the certified values (+1.95 and −2.20‰) within the above precision ranges.

4. Biostratigraphy

The upper Cenomanian to lower Turonian interval is traditionally characterized by three planktic foraminiferal biozones:

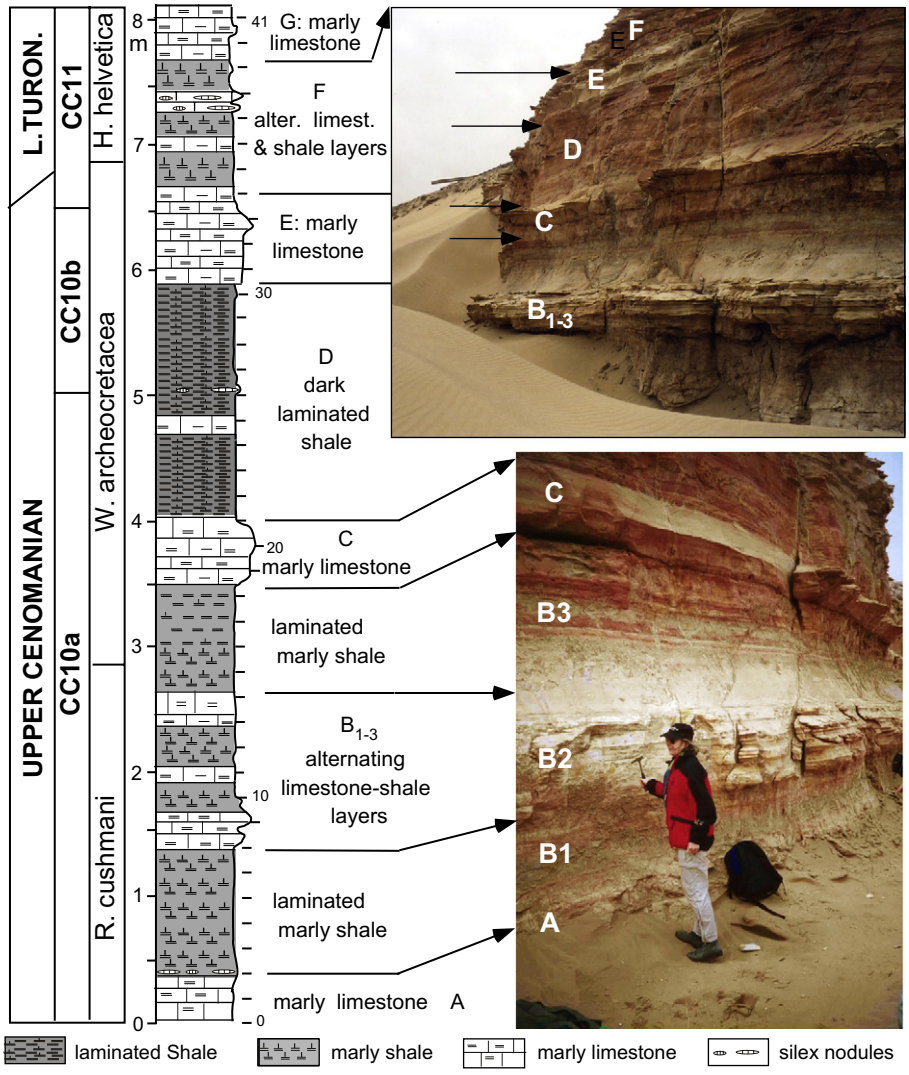

Fig. 3. Litholog and sedimentary units of the Tazra section keyed to outcrop photos. Planktic foraminiferal zones from this study, nannofossil zones from Tantawy (in this issue).

Rotalipora cushmani, *Whiteinella archeocretacea*, and *Helvetoglobotruncana helvetica* (Robaszynski and Caron, 1979). These biozones have provided useful age control worldwide. However, the increasingly detailed studies of the late Cenomanian anoxic event, biotic turnover, and $\delta^{13}C$ shift call for higher resolution age control. Based on a quantitative faunal study of Eastbourne, England, Keller et al. (2001) proposed a three-part subdivision of the *W. archeocretacea* biozone. Further refinement was proposed based on the C-T stratotype (GSSP) at Pueblo, Colorado, by subdividing the *R. cushmani* and *W. archeocretacea* zones into six subzones (Fig. 4), which in addition to the standard biozonation, mark the first $\delta^{13}C$ shift, the second $\delta^{13}C$ peak, the maximum expansion of the oxygen minimum zone (OAE), and the benthic oxic zone (Keller and Pardo, 2004a). Highest age resolution and the best correlation can be achieved by combining this refined zonal scheme with the $\delta^{13}C$ curve and oceanic events. This will not only provide two independent correlation proxies, one biotic and the other geochemical, but also a framework within which to judge the synchroneity of the $\delta^{13}C$ excursion, anoxic and oxic events across this critical interval.

The *Rotalipora cushmani* zone spans from the middle Cenomanian to the extinction of the nominate taxon shortly after the $\delta^{13}C$ excursion peak-1 in the uppermost Cenomanian. The uppermost part of this zone can be subdivided into two subzones, which mark the $\delta^{13}C$ shift (Fig. 4). The *Anaticinella multiloculata* subzone spans the interval from the first appearance of Whiteinella archeocretacea to the last occurrence of *Rotalipora greenhornensis*. In the Pueblo section, the nominate taxon is most abundant at the top of this subzone and near the onset of the $\delta^{13}C$ excursion. In this interval, *A. multiloculata* peaks in morphologic diversity showing gradations from its ancestor *R. greenhornensis* to *A. multiloculata* by loss of the keel and chamber inflation, probably in adaptation to living at shallower depths due to changes in the watermass stratification (e.g., expanding oxygen minimum zone, Eicher, 1972; Leckie, 1985; Desmares et al., 2003; Keller and Pardo, 2004a). In the Tazra section, *A. multiloculata* and its morphologic adaptations are common in the >250 μm size fraction near the top of the range of *R. greenhornensis* and up to the *R. cushmani* extinction. They are rare in the *W. archeocretacea* zone (Fig. 5). Until recently, *A. multiloculata* was only reported from Pueblo and other sequences in the Western Interior Seaway, but now has also been observed in the Wadi Bahloul section in Central Tunisia (Accarie et al., 1996). Their presence in the Tarfaya Basin confirms the global adaptation of this group to the oceanographic changes associated with the $\delta^{13}C$ excursion and OAE2.

The *Rotalipora* extinction subzone spans from the extinctions of *R. greenhornensis* at the base to the extinction of *R. cushmani* at the top; this subzone thus marks the extinction of all rotaliporids. In

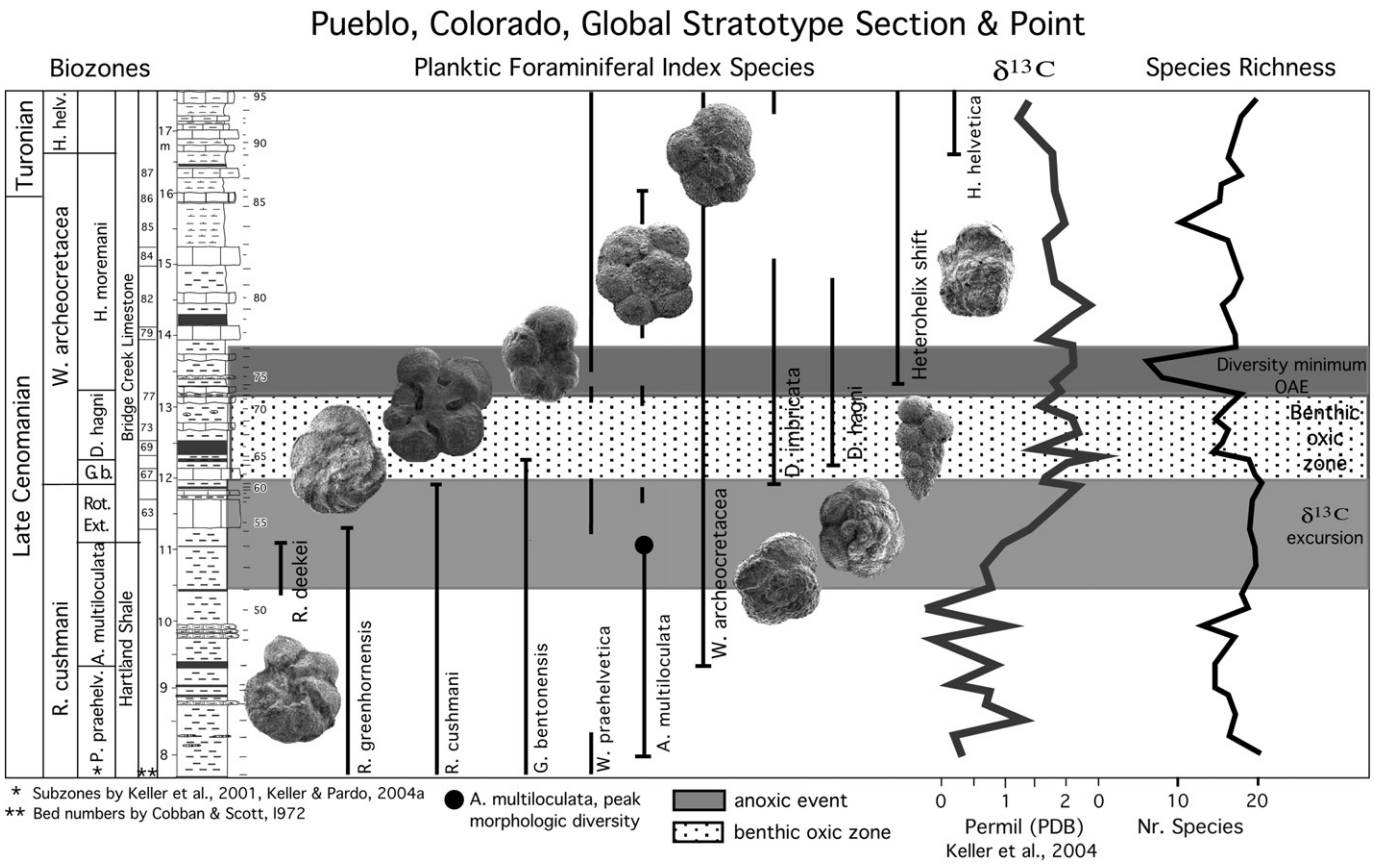

Fig. 4. High-resolution planktic foraminiferal biozonation of the upper Cenomanian to early Turonian, the $\delta^{13}C$ curve and species richness at the Pueblo, Colorado, Global Stratotype Section and Point (GSSP). The $\delta^{13}C$ excursion, benthic oxic zone, diversity minimum and oceanic anoxic event (OAE) mark prominent marker horizons.

continuous sequences, this subzone spans from near the base of the $\delta^{13}C$ excursion to the middle of the trough between two $\delta^{13}C$ peaks. At Pueblo the uppermost interval of this biozone is not present because of a short hiatus (Fig. 4). At Eastbourne, the last *R. cushmani* are observed within the trough about 20–70 cm above $\delta^{13}C$ peak-1 (Keller et al., 2001; Tsikos et al., 2004). In the Tarfaya basin, the base of the subzone is near the onset of the $\delta^{13}C$ excursion and the top is between 0.8 to 1.2 m above the $\delta^{13}C$ peak-1 based on studies by Luderer and Kuhnt (1997), Tsikos et al. (2004) and Kuhnt et al. (2004). At Tazra *R. cushmani* disappears about 90 cm above $\delta^{13}C$ peak-1 (Fig. 5).

The *Whiteinella archeocretacea* zone spans the interval from the *Rotalipora cushmani* extinction to the first appearance of *Helvetoglobotruncana helvetica*, which encompasses the critical interval from the trough between the two $\delta^{13}C$ peaks through the oxic and anoxic events to the Cenomanian/Turonian boundary. This zone is subdivided into three subzones to provide greater age control for this critical interval (Fig. 4). The *Globigerinelloides bentonensis* subzone defines the interval from the extinction of *R. cushmani* to the last appearance of the nominate taxon. This interval marks the trough between the two $\delta^{13}C$ excursions at Eastbourne, Pueblo and Tazra (Fig. 5).

The *Dicarinella hagni* subzone defines the interval from the last *G. bentonensis* to the onset of dominant *Heterohelix* species, termed the "*Heterohelix* shift" by Leckie et al., 1998). The *D. hagni* subzone encompasses the $\delta^{13}C$ peak-2 at Eastbourne and is condensed at Pueblo (Fig. 4). In the Tazra section, the $\delta^{13}C$ peak-2 is either missing or of very low amplitude due to diagenetic alteration (Fig. 5), and the *G. bentonensis* subzone is juxtaposed with the *Heterohelix* shift. This suggests that the *D. hagni* subzone and $\delta^{13}C$ peak-2 may be missing, or that the Heterohelix shift begins earlier in the Tarfaya basin. This latter possibility is discussed in the next section.

The *Heterohelix moremani* subzone defines the interval from the abrupt shift to *Heterohelix* dominated (60–90%) assemblages at the base to the first appearance of *Helvetoglobotruncana helvetica* at the top. The *Heterohelix* shift is a reliable global biomarker that reflects the expansion of the oxygen minimum zone after peak-2 of the $\delta^{13}C$ excursion. This biomarker has been reliably identified in various sections in Colorado (Leckie et al., 1998; Keller and Pardo, 2004a), at Eastbourne (Keller et al., 2001), in Tunisia (Nederbragt and Fiorentino, 1999), and now also in the Tarfaya Basin. However, the possibility of a diachronous onset of this anoxic event in the world oceans cannot be excluded.

The base of the *Helvetoglobotruncana helvetica* zone is defined by the first appearance of the nominate taxon, which occurs close to the Cenomanian-Turonian boundary as defined by the ammonite *Watinoceras devonense*. However, this species has been a problematic biomarker horizon for two major reasons. (1) It is difficult to separate *H. helvetica* morphotypes from its evolutionary ancestor *W. praehelvetica*. (2) These morphotypes are often rare or absent in the critical interval. At Tazra, *H. helvetica* first appears about 1 m above the peak OAE interval that is characterized by dark laminated shales and the planktic foraminiferal diversity minimum.

5. Placement of the Cenomanian/Turonian boundary

The C-T boundary is defined by the first occurrence (FO) of the ammonite *Watinoceras devonense* at the base of bed 86 in the Pueblo, Colorado, stratotype (Kennedy and Cobban, 1991; Kennedy et al., 2000). Among planktic foraminifera, the FO of

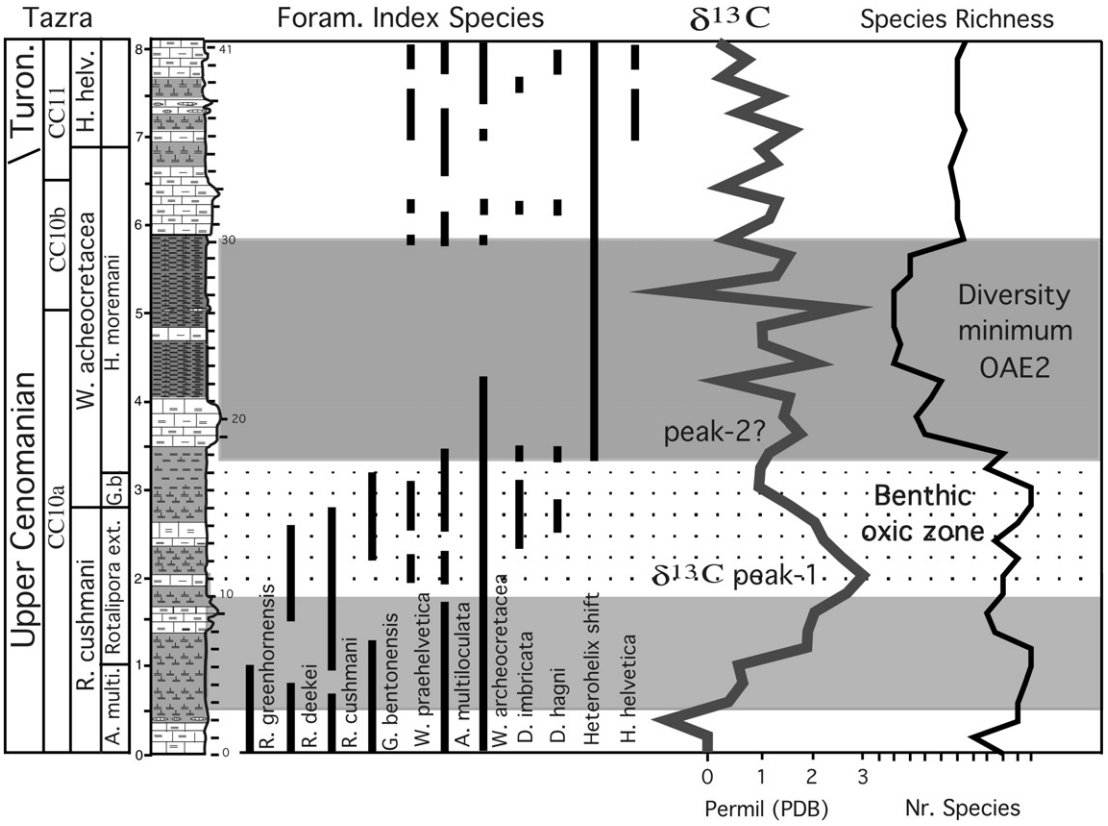

Fig. 5. Planktic foraminiferal zones, species richness and $\delta^{13}C$ curve across the Cenomanian-Turonian transition at the Tazra section, Tarfaya Basin, southwestern Morocco. Nannofossil zones from Tantawy (in this issue). Grey intervals mark $\delta^{13}C$ excursion, and diversity minimum. Stipled interval marks benthic oxic zone. Note the *D. hagni* subzone and the $\delta^{13}C$ peak-2 are not present at Tazra, suggesting a short hiatus.

Helvetoglobotruncana helvetica is a short interval (~90 cm) above the ammonite index species and close to the FO of the nannofossil *Quadrum gartneri* at both Pueblo and Eastbourne (Burnett, 1996; Keller et al., 2001; Keller and Pardo, 2004a). The $\delta^{13}C$ excursion gradually returns to pre-excursion values at or near the C/T boundary.

Placement of the C/T boundary in the Tarfaya sections is somewhat problematic. Ammonites are rarely present and reported from well above the $\delta^{13}C$ plateau, as well as the FO of *H. helvetica*, which suggests a delayed appearance of both index species relative to Pueblo. However, the FO of the nannofossil *Quadrum gartneri* is observed at or near the top of the $\delta^{13}C$ plateau in subsurface wells and therefore has been used as C/T marker by previous workers. We follow this practice at Tazra where the planktic foraminiferal index species *H. helvetica* first appears about 45 cm above the FO of *Q. gartneri* (Tantawy, in this issue Fig. 5). Although *H. helvetica* is rare, there seems to be no significant delay in its first appearance at Tazra.

6. Biotic turnover

Quatitative foraminiferal analysis of the Tazra section reveals that low diversity high-stress assemblages characterized the Tarfaya Basin during the late Cenomanian to early Turonian (Fig. 6), similar to Pueblo, Colorado (Leckie, 1985; Leckie et al., 1998; Keller and Pardo, 2004a; Keller et al., 2004). Species diversity in the upper *R. cushmani* zone (*A. multiloculata* and *Rotalipora* extinction subzones) varied between 15 and 20 species, with only five species common in the >63 μm size fraction. At Tazra, species richness dropped to 2 species in the anoxic interval and recovered to 10 species above it. This prolonged drop in species richness during the OAE2 is not observed at either Pueblo or Eastbourne, which suggests a higher stress environment in the Tarfaya Basin. Two species dominate the sequence throughout the studied interval. Below the OAE2 interval, *Hedbergella planispira* dominates (30–60%) along with *Heterohelix moremani* (20–48%), common *H. simplex* (5–14%), *W. arecheocretacea* (<10% except for one sample) and an incursion (5–25%) of *Guembelitria* (Fig. 6, Table 1). Above OAE2, *H. planispira* is dramatically reduced and replaced by almost exclusive dominance of *Heterohelix moremani* (80–100%). All other species are rare with sporadic occurrences.

The *Guembelitria* incursion at Tazra is of particular interest as it coincides with the only interval of common benthic species, all of which are low oxygen tolerant, and with minimum abundance of *Heterohelix* (Fig. 6) following the $\delta^{13}C$ excursion. A coeval interval with thes same characteristic was observed in the Pueblo section and termed "benthic oxic zone" (Eicher, 1969; Eicher and Worstell, 1970) because of the unique short-term appearance of low oxygen tolerant benthic species preceding the OAE2 (Keller and Pardo, 2004a). Although "benthic oxic zonet" seems like an oxymoron for a low oxygen tolerant assemblage, it is an appropriate term because it signals an influx of more oxic waters in an otherwise anoxic bottom environment that does not support benthic assemblages. Recently, this benthic oxic zone was also recognized in subsurface wells of the Tarfaya Basin beginning near the maximum $\delta^{13}C$ peak-1 (Kuhnt et al., 2004; Wagner et al., 2004). The most rapid biotic turnover (extinctions and originations) occurs in this oxic interval in the Tarfaya Basin as well as at Pueblo. The OAE2 abruptly terminates this oxic event with maximum biotic stress conditions resulting in the lowest species diversity (Fig. 6). The oceanographic implications of this benthic oxic zone are discussed below.

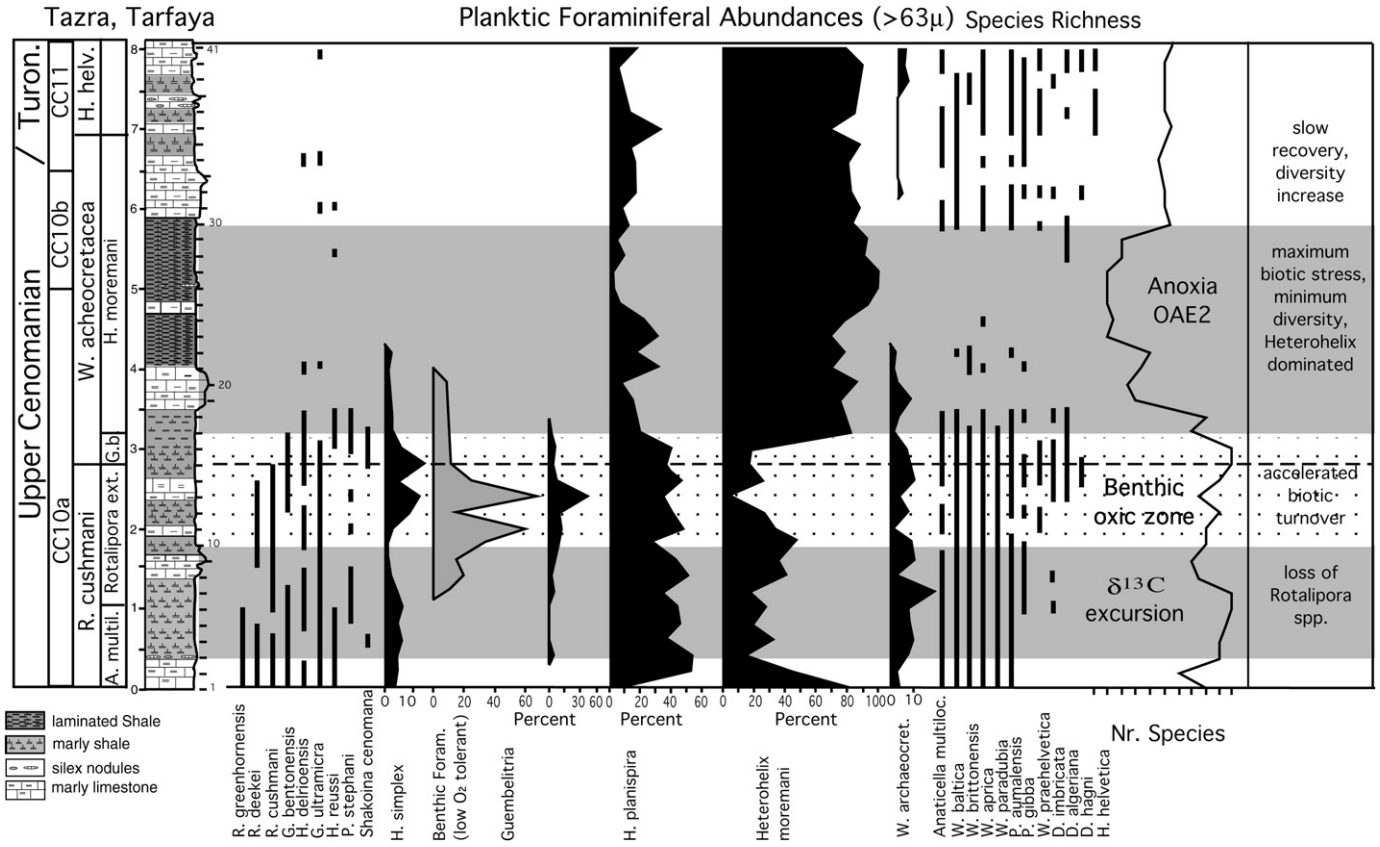

Fig. 6. Relative species abundances and diversity in planktic foraminifera across the C-T transition at Tazra, Tarfaya basin, Morocco. Nannofossil zones from Tantawy (in this issue). Planktic foraminifera responded to the initial rapid $\delta^{13}C$ excursion (grey interval) and the subsequent oxic zone (stippled) with a major biotic turnover replacing outgoing species with new evolving species. This oxic zone is also characterized by a *Guembelitria* incursion and abundant benthic foraminifera. The subsequent anoxic event (grey interval) resulted in a dramatic drop in species diversity to only 2 species. A slow recovery followed in the early Turonian.

7. Graphic correlation

How complete is the Tazra Tarfaya record? We applied the refined foraminiferal zonal scheme of the Pueblo stratotype to the Tazra section of the Tarfaya Basin. Compared with Pueblo, the *R. cushmani* extinction datum appears well after the $\delta^{13}C$ peak-1, as also observed in other Tarfaya sections (Luderer and Kuhnt, 1997; Tsikos et al., 2004; Kuhnt et al., 2004). Kuhnt et al. (2001) estimated the sedimentation rates in the Tarfaya Wells S75 between 6.2 to 7.4 cm/ky, which distinguishes this area as the most expanded and continuous sequences worldwide. In contrast, sedimentation rates at Pueblo are estimated at 1.10 to 1.24 cm/ky (Keller et al., 2004; Sageman et al., 2006), which suggests that discrepancies between the Tarfaya and Pueblo records may be largely due to the condensed sedimentation and/or short hiatus in the latter. This can be tested in graphic correlation based on stable isotope and planktic foraminiferal datum events (Shaw, 1964; Hart and Leary, 1991).

Graphic correlation of the Tazra section with those at Pueblo and Eastbourne can reveal stratigraphic differences in these sections (Figs. 7a, b). This method plots the same datum events of one section against the other as they occur in the stratigraphic sequences. If both sections are complete, the correlation line should be diagonal. If an interval is missing, a vertical or horizontal line marks the hiatus in the particular section. In the Pueblo section, the *R. cushmani* extinction and the $\delta^{13}C$ peak-1 coincide at the same stratigraphic level, whereas at Tazra these two markers are 90 cm apart (Fig. 7a). The horizontal line between the two *R. cushmani* extinction markers suggest that this missing interval is a short hiatus at Pueblo, confirming our previous observation of this hiatus (Keller et al., 2004; Keller and Pardo, 2004a). The *G. bentonensis* subzone is present in both sections and thus forms the short diagonal correlation line. The next foraminiferal biomarker is the *Heterohelix* shift, which marks the onset of OAE2. In the Pueblo section, this shift occurs about 1 m above the *G. bentonensis* subzone, but at Tazra this shift is juxtaposed above it, suggesting that the *Dicarinella hagni* subzone is missing at Tazra (vertical line, Fig. 7a). A diagonal line connects the *Heterohelix* shift to the C-T boundary marked by the first appearance of *H. helvetica* and/or *Quadrum gartneri*, revealing no further stratigraphic discrepancies between the two sections.

Graphic correlation thus reveals a short hiatus, or condensed interval, in the Pueblo section between the two $\delta^{13}C$ excursions, but also suggests a short hiatus or condensed interval in the Tazra section with the *D. hagni* subzone missing (Figs. 5, 7a). An alternate interpretation is shown by the dashed line, which assumes that the Tazra section is complete, even though the $\delta^{13}C$ peak-2 is either missing due to a hiatus or diagenesis, very condensed, or of very low amplitude (Fig. 7a). In this case, we must assume very condensed sedimentation at Pueblo (agrees with observations) and a diachronous (earlier) occurrence of the *Heterohelix* shift at Tazra.

Graphic correlation between Tazra and Eastbourne also reveals some ambiguities with respect to $\delta^{13}C$ peak-2. Based on $\delta^{13}C$ (onset of excursion and peak-1) and planktic foraminiferal markers, there appears to be a hiatus with part of *G. bentonensis*

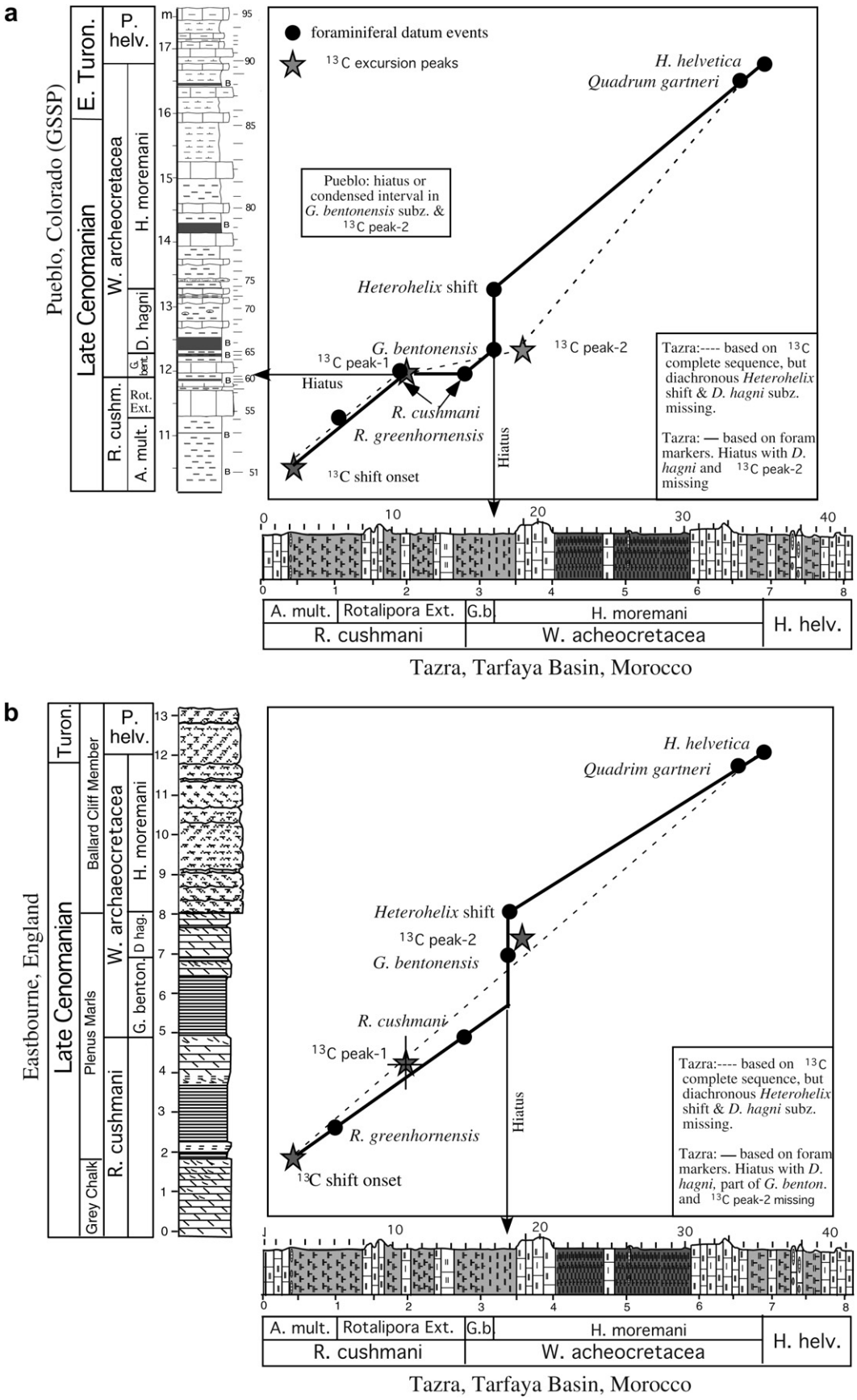

Fig. 7. a. Graphic correlation of the Pueblo, Colorado, and Tazra sections based on planktic foraminiferal index species and the $\delta^{13}C$ curve. Solid line marks correlation based on foraminiferal datums, dashed line is based on the onset of the $\delta^{13}C$ excursion and peaks-1 and 2. Based on foraminiferal datums, a short hiatus is indicated in the Pueblo section between $\delta^{13}C$ peaks 1 and 2, and a short hiatus may also be present in the Tazra (vertical line) in the lowermost *Whiteinella archeocretacea* zone. b. Graphic correlation of the Eastbourne, UK, and Tazra sections based on planktic foraminiferal index species and the $\delta^{13}C$ curve. Solid line marks correlation based on foraminiferal datums, dashed line is based on the onset of the $\delta^{13}C$ excursion and peaks-1 and 2. Based on foraminiferal datums, a short hiatus may be present in the Tazra section (vertical line) in the lowermost *Whiteinella archeocretacea* zone, as also noted by the absences of subzone *Dicarinella hagni*.

and *D. hagni* missing at Tazra (solid line, Fig. 7b). But, if we assume that Tazra is complete based on the $\delta^{13}C$ markers (dashed line), then the *R. cushmani* extinction and *Heterohelix* shift are both diachronous. Leckie (1985) and Leckie et al. (1998, p. 116) demonstrated that both of these events are diachronous in the U.S. western interior sea. At this time the assumption of a complete sequence at Tazra cannot be taken for granted and the possibility of diachronous biomarkers remains open. However, it appears that despite the very high sediment accumulation rate, the Tarfaya Basin experienced short intervals of erosion or non-deposition during $\delta^{13}C$ peak-2. This may be due to Tazra's location further inland and closer to the paleoshoreline, which likely experienced intermittent erosion. Kuhnt et al. (2004) suggested the presence of short hiatuses in this interval in the nearby subsurface cores (Fig. 1).

8. Stable isotopes

Carbon isotope values are relatively little affected by diagenetic processes (Schrag et al., l995) and should closely track environmental changes. Nevertheless, in depositional environments with anoxic bottom waters, such as the C-T transition, possible alteration of the primary isotopic signal due to the formation of early diagenetic carbonate must be considered. At Tazra, diagenetic alteration of the original carbonate is apparent in the ubiquitous infilling of foraminiferal tests by blocky calcite. In anoxic environments, pore-water may become easily oversaturated with respect to carbonate due to bacterial sulfate reduction. This leads to the formation of authigenic carbonates, which is depleted in ^{13}C due to the low $\delta^{13}C$ values of the precursory organic matter (e.g., Irwin et al., 1977; Coniglio et al., 2000; Raiswell and Fisher, 2004). Moreover, the isotope composition of oxygen in carbonates associated with organic matter scatters over a relatively large range (e.g., Mozley and Burns, 1993). Equilibration of HCO_3^- produced during sulfate reduction with seawater is considered to lead to roughly normal marine $\delta^{18}O$ values (e.g., Dickson et al., 2001; Raiswell and Fisher, 2004), whereas the frequently observed low $\delta^{18}O$ values (also found at Tazra, Fig. 8) may be explained by a model proposed by Sass et al. (1991). The presence of early diagenetic calcite depleted especially in ^{13}C was already suggested for other sections of the Tarfaya basin by Tsikos et al. (2004) and Kuhnt et al. (2004). This is supported by mineralogic analysis at Tazra (see below) where the presence of late diagenetic minerals implies a strong diagenetic overprint, which may explain the negative $\delta^{18}O$ values.

Despite diagenetic alteration of carbonate, especially in the surface outcrop at Tazra, a comparison of the $\delta^{13}C$carb record with nearby subsurface cores S57 and S75 shows nearly identical $\delta^{13}C$ excursion patterns, as well as long-term trends (Fig. 8). Thus, in the Tarfaya Basin the $\delta^{13}C$ record of bulk carbonate shows the characteristic positive excursion that is generally associated with enhanced organic carbon burial during a major oceanic anoxic event (Fig. 8, e.g., Arthur et al., 1987; Jenkyns et al., 1994; Mitchell et al., 1997). In wells S75 and S57 and the Tazra section, the $\delta^{13}C$carb excursion is about 3–4‰ and marks peak-1, followed by a rapid 2‰ decrease that marks the trough and the extinction of *R. cushmani*. However, the $\delta^{13}C$ peak-2 evident at Eastbourne is either missing or very reduced, showing an excursion of less than 1‰ (Fig. 8). Foraminiferal biostratigraphy and graphic correlations with Pueblo and Eastbourne suggest that $\delta^{13}C$ peak-2 may be missing due to a short hiatus in the Tarfaya Basin (Fig. 7a,b). Alternatively, the reduced and/or missing $\delta^{13}C$ peak-2 may be partly due to the formation of early diagenetic carbonate in anoxic bottom waters depleted in ^{13}C, which may decrease the $\delta^{13}C$ values of the bulk carbonate. However, diagenesis alone cannot explain the missing *D. hagni* biozone and the superposition of the *Heterohelix* shift and *G. bentonensis* subzone. Kuhnt et al. (2004), who also noted the significantly reduced (1‰) $\delta^{13}C$ peak-2 in well S75, suggested the presence of one or two short hiatuses in this interval.

Above this interval bulk carbonate $\delta^{13}C$ values gradually decrease into the lower Turonian, though with erratic 1–3‰

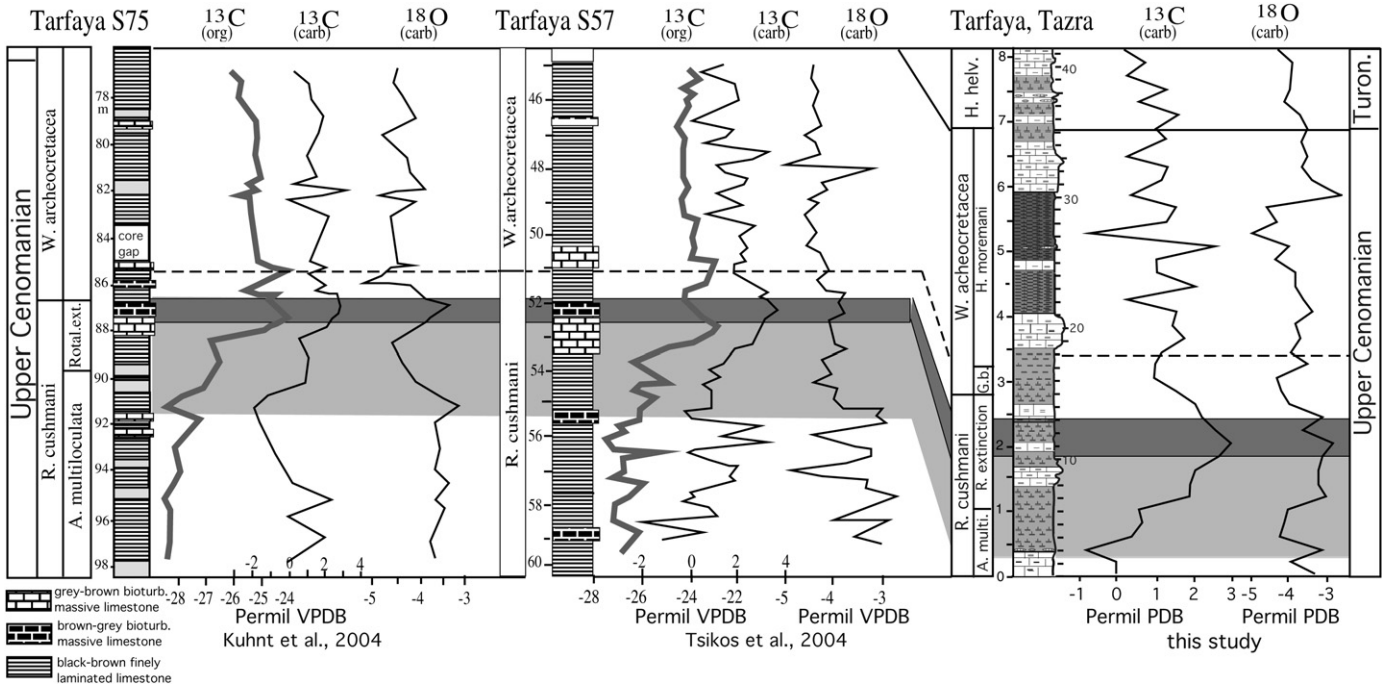

Fig. 8. Comparison of oxygen and carbon isotope curves at Tazra and nearby wells S75 and S57 shows δ^{13}Corg peak-1 predates the δ^{13}Ccarb peak-1 and δ^{13}Ccarb peak-2 is either missing due to a short hiatus (subzone *D. hagni*), or obscured due to diagenetic alteration.

fluctuations that are likely related to the formation of early diagenetic carbonate in anoxic bottom waters. Kuhnt et al. (2004) suggest that the fluctuations may be partly related to nutrient-rich upwelling during organic-rich periods.

Bulk rock $\delta^{13}C$ records at Tazra and wells S75 and S57 differ significantly from the $\delta^{13}C$org curves (Fig. 8). Major differences include the presence of the two-peak $\delta^{13}C$org excursion, but only peak-1 in $\delta^{13}C$carb noted above, and the offset between $\delta^{13}C$org and $\delta^{13}C$carb peaks. Kuhnt et al. (2004) estimate that $\delta^{13}C$org peaks predate $\delta^{13}C$carb peaks by about 15 ky in the Tarfaya Basin. A similar decoupling was observed by Mort et al. (2007) based on $\delta^{13}C$carb and phosphorus, with the latter preceding the $\delta^{13}C$ excursion by 30–60 ky in the most complete Tethyan sequences. Kuhnt et al. (2004) suggest that the decoupling of $\delta^{13}C$org may be due to photosynthesis of algae near the surface, which is less influenced by the upwelling nutrient cycle, which is the basis for $\delta^{13}C$carb. Mort et al. (2007) link it to the phosphorus cycle and the positive feedback between phosphorus sink and phosphorus source sustaining the productivity driven $\delta^{13}C$ excursion.

Original $\delta^{18}O$ values are not preserved in diagenetically altered sediments, such as at Tazra (see bulk rock mineralogy) and therefore calculated seawater temperatures do not reflect primary oceanographic signals. Nevertheless, temperature trends tend to be preserved (Schrag et al., l995). In the Tarfaya basin, the most positive $\delta^{18}O$ values coincide with the positive $\delta^{13}C$ excursion (Fig. 8) and suggest cool temperatures. Lighter $\delta^{18}O$ values in the trough and preceding the $\delta^{13}C$ peak-1 indicate warm periods. In the recovery phase after the $\delta^{13}C$ excursion, gradually increasing $\delta^{18}O$ values through the anoxic interval of the *W. archeocretacea* zone suggest climate cooling.

9. Total organic carbon

Organic carbon and Rock-Eval pyrolysis data indicate that average total organic carbon (TOC) values are very low, ranging from 0.015 to 0.1 (mean 0.05 wt%). TOC contents are lowest in the first 2 meters of the section, increase significantly just after the first $\partial^{13}C$ peak and reach a maximum near 2.8 m (Fig. 9a), Above this interval, TOC contents remain higher compared to the base of the section. TOC minima correspond to limestone intervals, whereas maxima correspond to laminated marlstones.

Information on the composition and maturity of organic carbon can be achieved by pyrolytic measurements (Espitalié et al., 1986; Behar et al., 2001). With this method the type of organic matter is determined by the hydrogen index (HI) and oxygen index (OI), which approximate the H/C and O/C atomic ratios, respectively. Based on the observed range of HI-values (0 to 20 mg HC/g TOC) and OI-values (2500 to 3500 mg CO_2/g TOC), the organic matter of the Tazra section is primarily type III organic matter (Fig. 9b) (Espitalié et al., 1986). However, such anomalously high OI values indicate significant alteration and oxidation of organic matter, which makes the oxygen and hydrogen indexes unreliable. At Mohamed and Amma Fatma beaches, coeval intervals show a contrary trend to Tazra, with high HI and low OI indicating a marine source for the organic matter. It is therefore likely that the observed TOC increase in the upper part of the Tazra section may only be the remnants of the considerable organic matter accumulation due to low oxygen and enhanced preservation due to anoxia. Alternatively, the Tazra organic matter reflects the proximal location of this section. This is also indicated by the order of magnitude higher TOC accumulation in cores S75 and S57 only a short distance from the

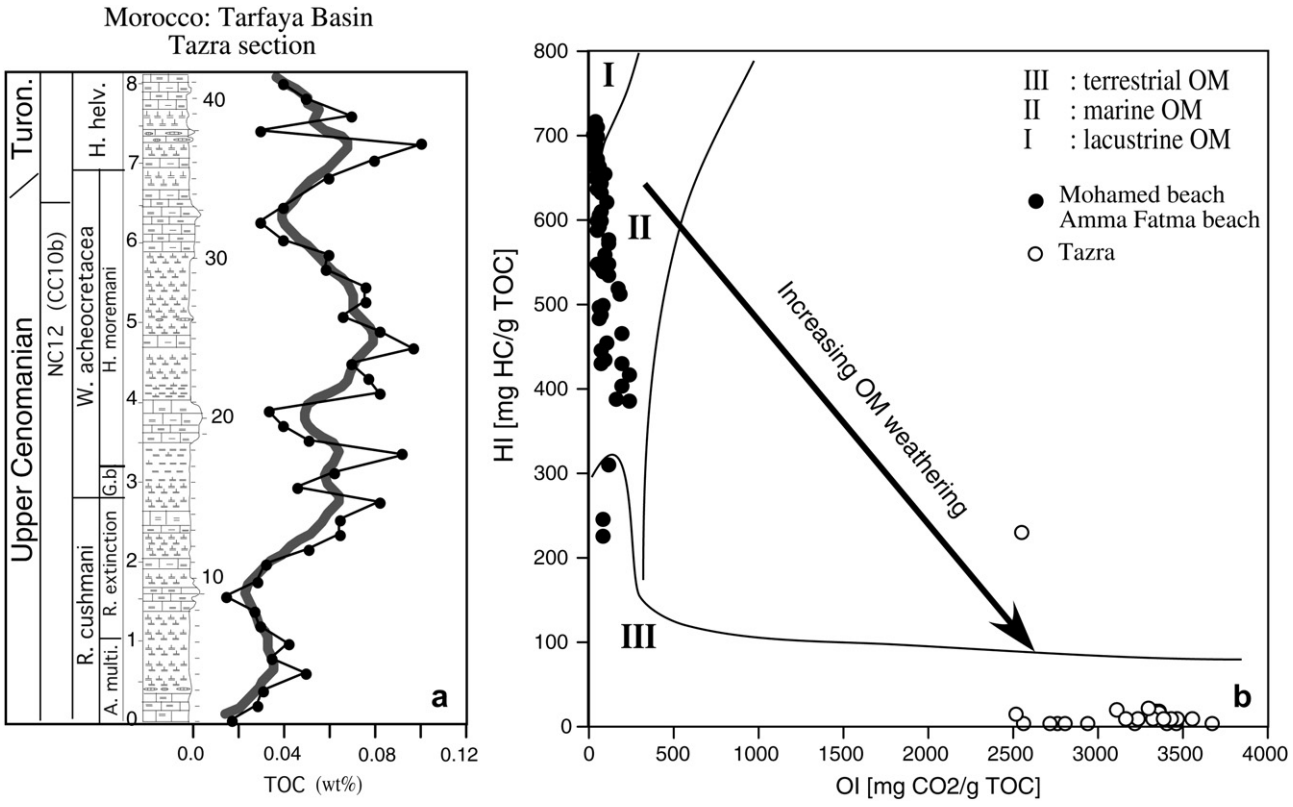

Fig. 9. a. TOC content of the Tazra section in the Tarfaya basin. Grey line marks 5-point average. Note that TOC contents increase just after the first ∂13C peak and remain significantly higher in the upper part of the section. The unusually low TOC values are a result of organic matter loss due to weathering. b. Hydrogen and oxygen index (HI, OI) in the Tazra section. Note the very low TOC and HI values but anomalously high OI values compared with nearby coeval sections at Mohamed and Amma Fatma beaches indicates deeply weathered organic matter at Tazra.

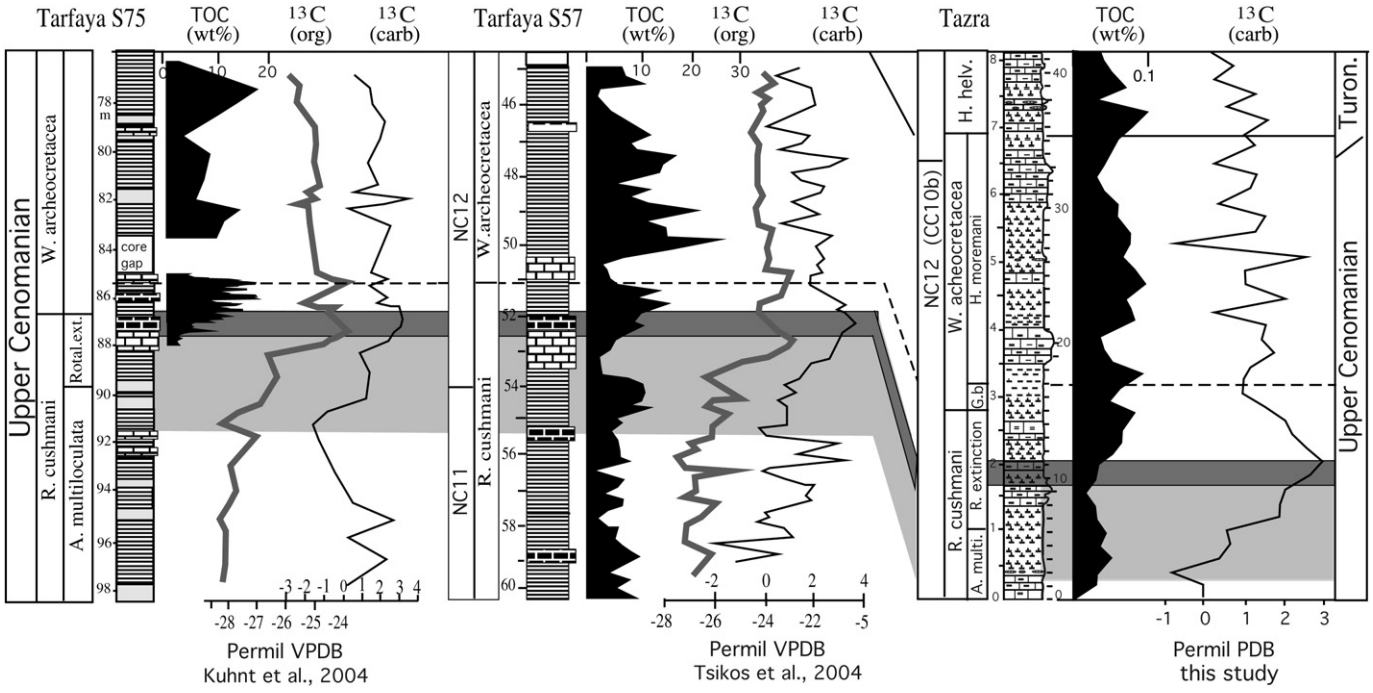

Fig. 10. Correlation of TOC, δ^{13}Corg and δ^{13}Ccarb curves at Tazra and nearby wells S75 and S57. Note that TOC values are very low at Tazra as a result of organic matter loss during weathering. Nevertheless, the TOC trend remains similar to trends at nearby wells S75 and S57.

Tazra section (Fig. 10, Kuhnt et al., 2004; Tsikos et al., 2004). Despite the low TOC accumulation rate at Tazra due to organic matter loss to weathering, the observed trends are correlateable.

10. Bulk mineralogy

The dominant bulk rock composition in the Tazra section consists of calcite (40–95%, mean 72%) with lower amounts of phyllosilicates (1–12%, mean 5%) and quartz (0.8–15%, mean 4%, Fig. 11). Lesser components include plagioclase and ankerite. Gypsum and halite, which originated from late diagenetic processes, are common and may reach 13% and 29%, respectively. This composition reflects the predominant marlstone lithology, which is enriched in phyllosilicates and quartz. Calcite maxima correspond to marly limestone and limestone layers. Major increases in detrital components (phyllosilicates, quartz and plagioclase), are observed in the marlstone intervals at 1.8 m, 4.2 m and 5.8 m, respectively.

The calcite/detritus ratio [C/D = calcite/(quartz + phyllosilicates + feldspars)] is generally quite high and reflects low detrital input (Fig. 11). High C/D ratios suggest repeated periods of weak continental runoff, whereas lower C/D ratios indicate increased

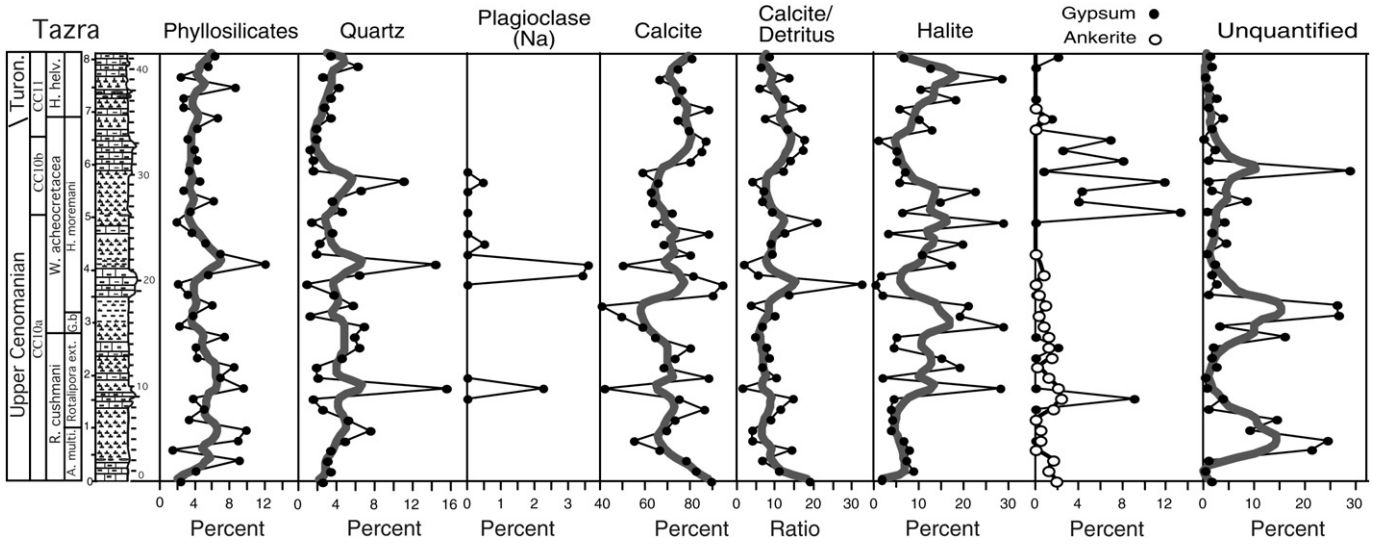

Fig. 11. Bulk rock composition in the Tazra section. The dominant components are calcite, quartz and phylloslicates. Grey lines mark 5-point average. Note the overall high calcite/detritus (C/D) ratio indicates reduced detrital input, especially in marly limestone and limestone intervals. Marly layers show lower C/D ratios and reflect higher detrital input due to increased continental runoff.

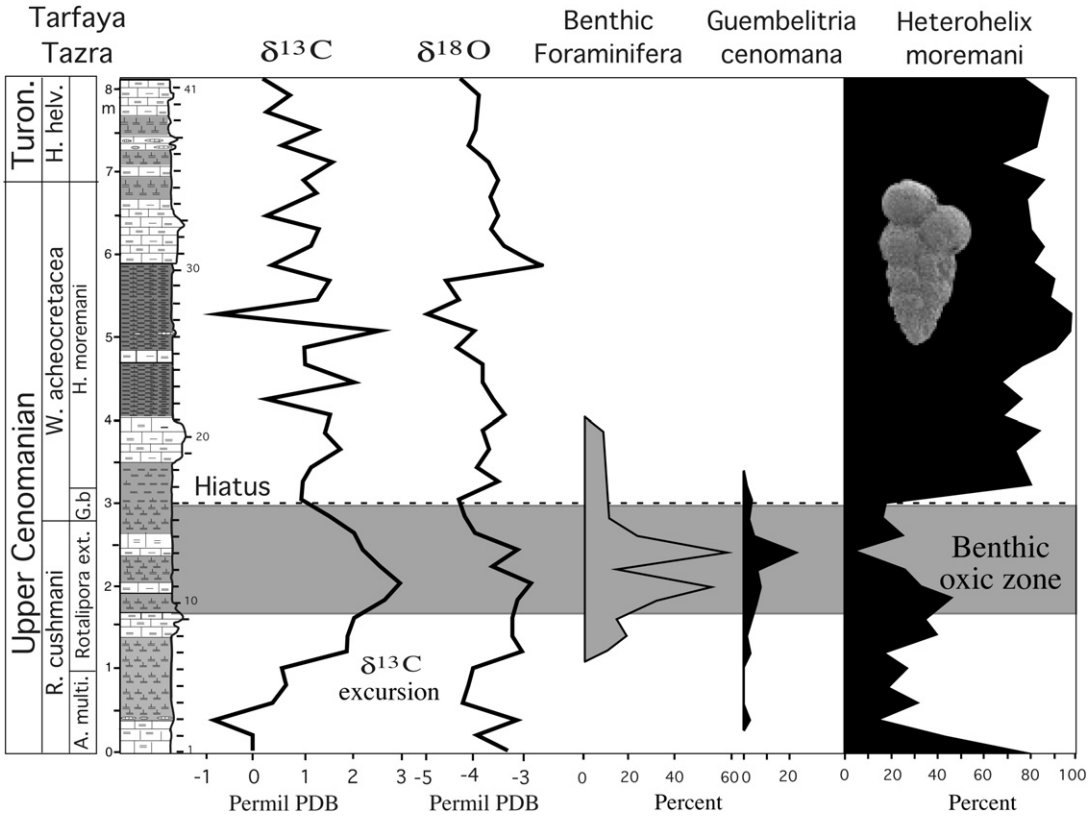

Fig. 12. The $\delta^{13}C$ excursion at Tazra, Tarfaya basin, is characterized by an oxic zone, which marks intense upwelling of nutrient-rich deeper water prior to the anoxic event OAE2. A similar oxic zone is present at Pueblo. The oxic zone is marked by abundant benthic foraminifera and an influx of *Guembelitria*.

runoff linked to increased humidity on the Western African margin and/or proximity to the shoreline. The oxic zone interval, recognized based on benthic and planktic foraminifera (Fig. 6), corresponds mainly to lower C/D ratios and hence increased continental runoff. Observed fluctuations in aridity and humidity over West Africa are likely due to Milankovitch-forced variations in insolation, as supported by global climate models of the C-T transition (Flögel, 2002; Kolonic et al., 2005). Late diagenetic minerals, such as gypsum, halite and ankerite, may account for more than 30% of the bulk mineralogy. These minerals are prevalent from 1.5 m to the top of the section. Gypsum is abundant between 5.0 m and 6.5 m. The presence of these late diagenetic minerals implies a strong diagenetic overprint, which may explain the negative $\delta^{18}O$ values observed at Tazra (Fig. 8).

11. Discussion

11.1. Duration of OAE2

The Tarfaya sedimentary record across the late Cenomanian to early Turonian oceanic anoxic event (OAE2) is one of the most complete worldwide and it is comparable with the Pueblo stratotype in the US and the Eastbourne section in the UK, though with a higher rate of sediment accumulation. The OAE2 interval can be globally recognized based on the rapid positive $\delta^{13}C$ excursion and plateau of high values up to the C/T boundary, followed by a gradual return to pre-excursion values. At Tarfaya, the duration of the entire $\delta^{13}C$ excursion is estimated at 440 ky by Kuhnt et al. (2004) and 490 ky by Kolonic et al. (2005) based on cyclic sedimentation, which is interpreted as response to orbital forcing and assuming constant sedimentation rates. These age estimates are close to the ~500 ky duration estimated from the US Western interior based on cyclic sedimentation and radiometric dating (Obradovich, l993; Sageman et al., 1998, 2006; Meyers et al., 2001, 2005; Keller and Pardo, 2004a).

The oceanic anoxic event, represented by black shale accumulation, may coincide with or postdate the initial $\delta^{13}C$ excursion. Different definitions of what constitutes the OAE2 interval, the duration of anoxic sedimentation, and the duration of the isotopic excursion can account for some of the difference. Recent high-resolution stratigraphic and geochemical data from the most complete sequences shows that there is a lag time of 15–60 ky between the onset of anoxic sedimentation and the $\delta^{13}C$ excursion (Kuhnt et al., 2004; Mort et al., 2007).

11.2. Biotic effects of OAE

The OAE2 interval from the onset of the rapid $\delta^{13}C$ excursion through the plateau of high $\delta^{13}C$ values spans a series of biotic and oceanic events that are easily identified and provide insights into the changing environmental conditions and associated increasing biotic stress. Planktic foraminifera living in surface and subsurface waters are sensitive to environmental changes in temperature, salinity, oxygen and nutrients. They respond strongly to changes of the OAE2 by species extinctions, evolutionary diversification, morphological adaptations, prolonged absence of species and changes in the relative abundance of species populations (Leckie, 1985; Hart and Ball, 1986; Hart and Leary, 1991; Hart, 1996; Luderer and Kuhnt, 1997; Price et al., 1998; Leckie et al., 2002; Keller et al., 2001; Keller and Pardo, 2004a). However, this biotic turnover is not a major mass extinction as most species survived in refugia and returned when conditions improved. The biotic effects vary across latitudes,

paleodepth and paleogeographic regions as a direct response to the severity of the OAE2.

For example, the biotic response of planktic foraminifera to the OAE2 is stronger in the Tarfaya Basin than at Pueblo or Eastbourne (Fig. 6). At Tazra, the evolutionary turnover has four distinct stages: (1) the loss of rotaliporids associated with the $\delta^{13}C$ excursion; (2) accelerated turnover associated with the influx of oxic bottom waters during the maximum $\delta^{13}C$ excursion; (3) maximum biotic stress expressed by minimum species diversity and shift to *Heterohelix* dominated assemblages after the oxic bottom water event; and (4) recovery after OAE2. These four stages can be generally recognized throughout the Tethys, but are particularly well defined at Tazra in the Tarfaya Basin probably due to more extreme biotic stress associated with the upwelling region and high organic input off northwest Africa.

11.2.1. Stage 1: loss of rotaliporids during $\delta^{13}C$ excursion

During the $\delta^{13}C$ excursion the last single keeled rotaliporids, as well as some other species, disappeared and were replaced by dicarinellids. This one-for-one replacement resulted in no overall net loss in species diversity, as also observed at Pueblo and Eastbourne (Keller et al., 2001; Keller and Pardo, 2004a). Both outgoing and incoming species were relatively rare and minor components of the total planktic foraminiferal population in the $>63\ \mu$ size fraction. But during the $\delta^{13}C$ excursion prior to their extinction (*A. multiloculata* and *Rotalipora extinction* subzones) rotaliporids experienced a burst of morphological diversification, leading to changes in the number and shape of chambers, the weakening of keels in formerly thickly keeled species (*R. cushmani*, Luderer and Kuhnt, 1997) and even the nearly complete loss of keels by formerly strongly keeled species (*R. greenhornensis* transition to *Anaticella multiloculata*) possibly as a result of adaptation to living in shallower waters. Whiteinellids also experienced a burst of morphological change.

This morphologic diversification appears to have been a response to increasingly stressful environmental conditions that included changes in watermass stratification, increased upwelling and nutrient supply, higher surface productivity and an expanded oxygen minimum zone. For most species this adaptation strategy failed, perhaps because of rapidly changing environmental conditions with the influx of oxic deep waters and changing watermass stratification. Dicarinellids evolved and successfully adapted to the new conditions, and their competition probably hastened the demise of the rotaliporids. The surface dweller *Hedbergella planispira*, which is tolerant of salinity fluctuations (Keller and Pardo, 2004a) and the low oxygen tolerant *Heterohelix moremani* thrived (Fig. 6).

11.2.2. Stage 2: accelerated turnover, upwelling and oxic waters

During the maximum $\delta^{13}C$ excursion the evolutionary turnover accelerated coincident with intensified upwelling and an influx of oxic bottom waters, which for a brief time established diverse benthic assemblages where none survived before or after. The low oxygen tolerant *Heterohelix* populations dramatically decreased in response to more oxygenated waters throughout the water column, *Guembelitira* thrived and the surviving rotaliporid species rapidly disappeared (Figs. 6, 12). This interval of accelerated extinctions and oxic waters reflects an unusual interlude in the long-term trend toward oceanic anoxia during the latest Cenomanian and may be related to cooling and a lower sea level. In the Tarfaya basin, the benthic oxic zone is recognized at Tazra, as well as in subsurface wells, beginning near the maximum $\delta^{13}C$ peak-1 (Luderer and Kuhnt, l997; Kuhnt et al., 2004; Wagner et al., 2004) and continuing up to the *Heterohelix* shift.

The oxic zone and *Guembelitria* incursion marks an important and widespread oceanographic and climatic event that is also observed at Pueblo (Fig. 13). Although Leckie (1985) and Leckie et al. (1998) reported relatively low values (<10%) in the Rock Canyon, Pueblo section, they observed peak values of >80% in the correlative interval at their shallower Lohali Point section on the southwestern side of the seaway. This indicates that *Guembelitria* blooms are common in shallow nearshore areas. Analogous *Guembelitria* blooms during the late Maastrichtian and Cretaceous-Tertiary (K-T) transition mark high stress conditions in eutrophic surface waters in upwelling areas and near continental

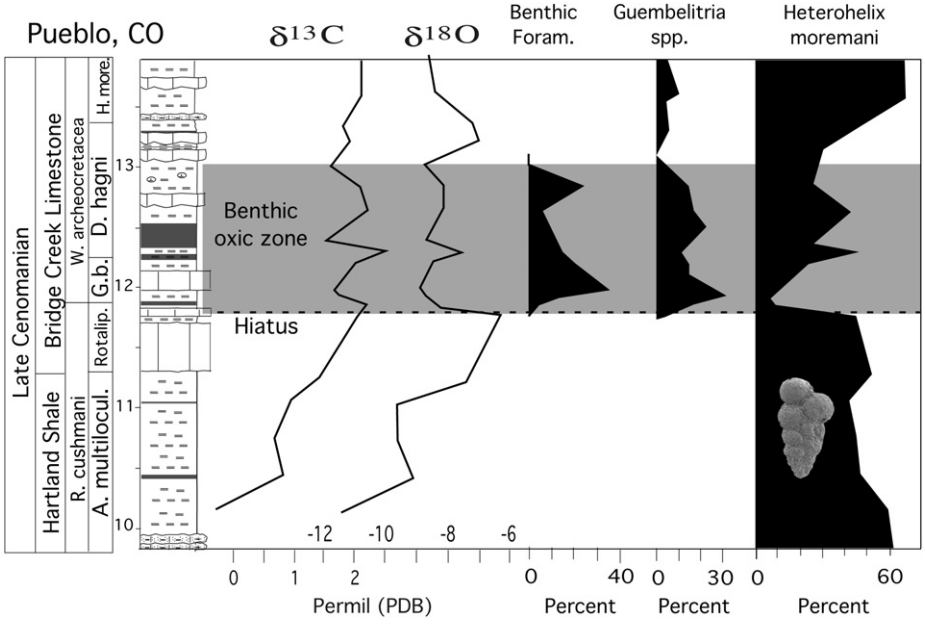

Fig. 13. The $\delta^{13}C$ excursion at Pueblo, Colorado is characterized by an oxic zone, which marks upwelling of oxygen and nutrient-rich deeper water prior to the anoxic event OAE2. The oxic interval is marked by the presence of common benthic foraminifera on the seafloor where there were none before and after, a dramatic decrease in *Heterohelix* species indicating an oxic water column, and an influx of *Guembelitria* in surface waters.

margins (Koutsoukos, l996; Keller, 2003; Keller and Pardo, 2004b; Pardo and Keller, in this issue). Similar to the late Maastrichtian and K-T transition, *Guembelitria* influx during the OAE2 $\delta^{13}C$ excursion at Tazra suggests nutrient-rich surface waters due to upwelling and/or increased influx of nutrients from continental areas due to climate change. Mineralogical analysis provides evidence for increased continental runoff during the oxic zone interval, as indicated by lower calcite/detritus (C/D) ratios (Fig. 11). Stable isotopes indicate that this interval marks peak cooling, which suggests upwelling of cool oxygen- and nutrient-rich waters, as well as increased runoff (Fig. 8).

The benthic oxic zones at Tazra and Pueblo appear to be diachronous, although this seems to be an artifact of the variable sedimentation rates and hiatus patterns (Figs. 7a,b). For example, the pronounced post $\delta^{13}C$ peak-1 decrease evident at Tazra is missing at Pueblo, whereas the subsequent *D. hagni* subzone present at Pueblo is missing at Tazra. Once the correlation is adjusted for these stratigraphic gaps, the benthic oxic zone appears essentially coeval, but seems to have started earlier and with more intensity along the Atlantic coast bordering the Tarfaya basin than in the US Western Interior. Slightly different timing and intensity of upwelling should be expected in such widely differing settings as the US Western Interior and the Moroccan Atlantic margin.

11.2.3. Stage 3: maximum biotic stress and oceanic anoxia

Oxygenation of the water column was rapidly replaced by global oceanic anoxia and maximum biotic stress. The anoxic event is easily recognized in shelf and deep marine sequences by laminated black organic-rich shale deposition and is usually referred to as OAE2 in the narrow sense. The biotic stress associated with this event appears to have been particularly severe in the Tarfaya Basin. Species richness dropped to just two species (*Heterohelix* subzone), with *Heterohelix moremani* dominating (80–100%) and *Hedbergella planispira* decreasing dramatically (Fig. 6). At Tazra, the abrupt nature of this change is partly an artifact of the hiatus between *G. bentonensis* and *Heterohelix* subzones, though a similarly abrupt onset to near total dominance by *Heterohelix* species has been observed in the US Western Interior Seaway (Leckie et al., 1998; Keller and Pardo, 2004a), Eastbourne, UK (Keller et al., 2001) and Tunisia (Nederbragt and Fiorentino, 1999), The *Heterohelix* shift is thus a global marker for the OAE2. The extremely low species richness in the Tarfaya Basin is associated with maximum organic matter accumulation and anoxic sea floor as indicated by the absence of benthic foraminifera. Low oxygen conditions apparently prevailed throughout the water column as suggested by the presence of only low O_2 tolerant heterohelicids and reduced populations of *Hedbergella planispira* in surface waters.

The biotic stress of the OAE2 varies across latitudes, and across shelf to open ocean environments, but no systematic analysis has been done to date. In some deep-water sequences, the black organic-rich shale associated with this anoxic event contains no calcareous microfossils (e.g., Italy, Luciani and Cobianchi, 1999). In continental shelf environments the reduction in calcareous plankton diversity appears short-lived and/or much reduced, though it is unclear whether this is a function of high sedimentation rates, hiatus, or a shorter time interval of low oxygen conditions. (e.g., Eastbourne, England, Keller et al., 2001; Pueblo, CO, Keller and Pardo, 2004a; Sergipe Basin, Brazil, Koutsoukos et al., l990).

11.2.4. Stage 4: post OAE recovery

The return to a more oxygenated water column and reduced planktic stress begins in the upper part of the *W. acrcheocretacea* zone and prior to the C-T boundary. The recovery is expressed by sharply increased species diversity due to reappearing species rather than evolution, and less organic-rich laminated shales (Fig. 6). However, the reappearing planktic foraminiferal species (e.g., whiteinellids, dicarinellids, anaticellids, praeglobotruncanids) remain rare and sporadically present. In contrast, the low oxygen tolerant *Heterohelix* group remains dominant (80–90%) and virtually unchanged. This suggests that the oxygen minimum zone remained very expanded, thereby reducing niche space for returning species requiring well-oxygenated waters, well into the early Turonian in the Tarfaya Basin. Continued dominance of *Heterohelix* into the early Turonian is ubiquitous in the Tethys Ocean and suggests a continued high flux of organic matter from the photic zone and/or sluggish oceanic circulation.

12. Summary and conclusions

The OAE2 interval from the onset of the rapid $\delta^{13}C$ excursion through the plateau of high $\delta^{13}C$ values spans a series of biotic and oceanic events that are easily identified and provide insights into the changing environmental conditions and associated increasing biotic stress. Planktic foraminifera respond strongly to changes in OAE2 by species extinctions, evolutionary diversification, morphological adaptations, prolonged absence of species and changes in the relative abundance of species populations. However, this biotic turnover is not a mass extinction as most species survived in refugia and returned when conditions improved. Biotic effects vary across latitudes, paleodepth and paleogeographic regions as a direct response to the severity of the OAE2. The planktic foraminiferal response to the OAE2 in the Tazra (Tarfaya Basin), Eastbourne (UK) and Pueblo, Colorado (USA) can be characterized in four stages, though the conditions may have been more extreme in the Tarfaya Basin.

(1) Rapid $\delta^{13}C$ excursion and onset of a biotic turnover with morphologic adaptation of rotaliporids (by weakening and loss of the keel, and chamber inflation) to living in shallower more oxygen-rich waters in response to expanding oxygen minimum zone (OMZ).
(2) Maximum $\delta^{13}C$ excursion (peak−1 to peak−2, *G. bentonensis* and *D. hagni* subzones) is marked by a major environmental change accompanied by intense upwelling of oxygenated, nutrient-rich deeper water. At this time, dicarinellids diversified, rotaliporids disappeared, low oxygen tolerant heterohlicids dramatically decreased, and *Guembelitria* invaded surface waters of the Tarfaya basin and benthic foraminifera thrived on the seafloor.
(3) Maximum stress conditions characterize the $\delta^{13}C$ plateau (lower part of *Heterohelix* subzone). At this time, species richness dropped to just two species at the Tazra section with *Heterohelix moremani* dominant (80–100%) and minor *Hedbergella planispira*. The extremely low species richness is associated with maximum organic matter accumulation, anoxic sea floor (absence of benthic foraminifera), and a very expanded oxygen minimum zone where only low O_2 tolerant heterohelicids thrived in the water column.
(4) Slow recovery and continued biotic stress characterize the upper part of the *Heterohelix* subzone up to the C/T boundary. During this time sharply increased species diversity, due to reappearance of species rather than evolution, and less organic-rich laminated shales suggest the return of more oxygenated water column and reduced biotic stress. *Heterohelix* remained dominant (80–90%), suggesting low oxygen conditions prevailed in subsurface waters into the early Turonian in the Tarfaya basin.

The OAE2 biotic turnover suggests that the stress on calcareous plankton was related to changes in the watermass

stratification, intensity of upwelling, nutrient flux and oxic levels in the water column driven by changes in climate and oceanic circulation. The ultimate cause for these environmental changes may have been the large igneous province volcanism, though the direct cause-and-effect relationship has yet to be demonstrated.

Acknowledgments

We are grateful for the thoughtful comments and critiques of the four reviewers, especially Mark Leckie and Malcolm Hart, whose insightful comments much improved this manuscript. This report is based upon work supported by the US National Science Foundation under Grant NSF INT 0115357 (GK), the Swiss National Fund No. FN21-67702.02 (TA), and the German Science Foundation grant STU 169/10-1 to 3 (DS).

References

Adatte, T., Stinnesbeck, W., Keller, G., 1996. Lithostratigraphic and mineralogical correlations of near-K/T boundary clastic sediments in northeastern Mexico: implications for mega-tsunami or sea level changes? Geological Society of America Special Paper 307, 197–210.

Accarie, A., Emmanuel, L., Robaszynski, R., Baudin, F., Amedro, F., Caron, M., Deconinck, J., 1996. Carbon isotope geochemistry as stratigraphic tool. A case study of the Cenomanian/Turonian boundary in central Tunisia. Comptes Rendus de l'Académie des Sciences Paris (2a) 322, 579–586.

Arthur, M.A., Schlanger, S.O., Jenkyns, H.C., 1987. The Cenomanian-Turonian oceanic anoxic event, II. Palaeoceanographic controls on organic-matter production and preservation. In: Brooks, J., Fleet, J.A. (Eds.), Marine Petroleum Source Rocks. Geological Society of London, Special Publication, vol. 26, pp. 401–420.

Banerjee, A., Boyajian, G., 1996. Changing biologic selectivity of extinction in the foraminifera over the past 150 m.y. Geology 24, 607–610.

Behar, F., Beaumont, V., De Pentadeo, B., 2001. Rock-Eval technology: performances and developments. Oil and Gas Science and Technology. Revue IFP 56 (2), 111–134.

Burnett, J.A., 1996. Nannofossils and Upper Cretaceous (sub-)stage boundaries – state of the art. Journal of Nannoplankton Research 18, 23–32.

Caron, M., 1985. Cretaceous planktonic foraminifera. In: Bolli, H.M., Saunders, J.B., Perch-Nielsen, K. (Eds.), Plankton Stratigraphy. Cambridge University Press, Cambridge, pp. 17–86.

Caron, M., Dall'Agnolo, S., Accarie, H., Barrera, E., Kauffman, E.G., Amedro, F., Robaszynski, F., 2006. High-resolution stratigraphy of the Cenomanian-Turonian boundary interval at Pueblo (USA) and wadi Bahloul (Tunisia): stable isotope and bio-events correlation. Geobios 39, 171–200.

Coniglio, M., Myrow, P., White, T., 2000. Stable carbon and oxygen isotope evidence of Cretaceous sea-level fluctuations recorded in septarian concretions from Pueblo, Colorado, U.S.A. Journal of Sedimentary Research 70, 700–714.

Crowley, T.J., 1991. Past CO_2 changes and tropical sea surface temperatures. Paleoceanography 6, 387–394.

Desmares, D., Grosheny, D., Beaudoin, B., 2003. Hétérochronies du dévelopment sensu Gould chez les foraminifères cénomaniens: exemple de néoténie dans le basin due Western Interior americain. Comptes rendus Palevol 2, 587–595.

Dickson, J.A.D., Montanez, I.P., Saller, A.H., 2001. Hypersaline burial diagenesis delineated by component isotopic analysis, late Paleozoic limestones, West Texas. Journal of Sedimentary Research 71, 372–379.

Eicher, D.L., 1969. Paleobathymetry of the Cretaceous Greenhorn Sea in eastern Colorado. American Association of Petroleum Geologists Bulletin 53, 1075–1090.

Eicher, D.L., 1972. Phylogeny of the Late Cenomanian planktonic Foraminifer *Anaticinella multiloculata* (Morrow). Journal of Foraminiferal Research 2, l84–190.

Eicher, D.L., Worstell, P., 1970. Cenomanian and Turonian foraminifera from the Great Plains, United States. Micropaleontology 16, 269–324.

El Albani, A., Kuhnt, W., Luderer, F., Herbin, J.P., Caron, M., 1999. Palaeoenvironmental evolution of the late Cretaceous sequences in the Tarfaya Basin (southwest of Morocco). In: Cameron, N.R., Bate, R.H., Clure, V.S. (Eds.), The Oil and Gas Habitats of the South Atlantic. Geological Society of London, Special Publication, vol. 153, pp. 223–240.

Erba, E., Tremolada, F., 2004. Nannofossil carbonate fluxes during the early Cretaceous: phytoplankton response to nutrification episodes, atmospheric CO_2, and anoxia. Paleoceanography 19, 1008, doi:10.1029/2003PA000884.

Espitalié, J., Deroo, G., Marquis, F., 1986. La pyrolyse Rock-Eval et ses applications. Partie 3. Revue IFP 41, 1.

Föllmi, K.B., Weissert, H., Bisping, M., Funk, H., 1994. Phosphogenesis, carbon isotope stratigraphy and carbonate-platform evolution along the lower Cretaceous northern Tethyan margin. Geological Society America Bulletin 106, 729–746.

Flögel, S., 2002. On the influence of precessional Milkankovitch cycles on the Late Cretaceous climate system: comparison of GCM results, geochemical, and sedimentary proxies for the western interior seaway of North America. PhD thesis, University of Kiel, Germany.

Gale, A.S., Jenkyns, H.C., Kennedy, W.J., Corfield, R.M., 1993. Chemostratigraphy versus biostratigraphy: data from around the Cenomanian – Turonian boundary. Journal of the geological Society, London 150, 29–32.

Gale, A.S., Smith, A.B., Monks, N.E.A., Young, J.A., Howard, A., Wray, D.S., Huggett, J. M., 2000. Marine biodiversity through the Late Cenomanian-Early Turonian: paleoceanographic controls and sequence stratigraphic biases. Journal of the Geological Society, London 157, 745–757.

Gale, A.S., Hardenbol, J., Hathway, B., Kennedy, J.W., Young, J.R., Phansalkar, V., 2002. Global correlation of Cenomanian (upper Cretaceous) sequences: evidence for Milankovitch control on sea level. Geology 30, 291–294.

Gebhardt, H., Kuhnt, W., Holbourn, A., 2004. Foraminiferal response to sea level change, organic flux and oxygen deficiency in the Cenomanian of the Tarfaya Basin, southern Morocco. Marine Micropaleontology 53, 133–157.

Hallam, A., 1992. Phanerozoic Sea Level Changes. Columbia University Press, New York.

Haq, B.U., Hardenbol, J., Vail, P.R., 1987. Chronology of fluctuating sea levels since the Triassic. Science 235, 1156–1167.

Harries, P.J., 1993. Dynamics of survival following the Cenomanian-Turonian (Upper Cretaceous) mass extinction event. Cretaceous Research 14, 563–583.

Hart, M.B., 1996. Recovery of the food chain after the Late Cenomanian extinction event. In: Hart, M.B. (Ed.), Biotic Recovery from Mass Extinction Events. Geological Society of America, Special Publication, vol. 102, pp. 265–277.

Hart, M.B., Ball, K.C., 1986. Late Cretaceous anoxic events, sea level changes and the evolution of the planktonic foraminifera. In: Summerhayes, C.P., Shackleton, N.J. (Eds.), North Atlantic Paleoceanography. Geological Society, Special Publication, vol. 21, pp. 67–78.

Hart, M.B., Bigg, P.J., 1981. Anoxic events in the Late Cretaceous chalk seas of northwest Europe. In: Neale, J.W., Brasier, M.D. (Eds.), Microfossils from Recent and Fossil Shelf Sea. British Micropaleontological Society. Ellis Horwood, Chichester, pp. 177–185.

Hart, M.B., Leary, P.N., 1989. The stratigraphic and paleoceanographic setting of the late Cenomanian "anoxic" event. Journal of the Geological Society, London 146, 305–310.

Hart, M.B., Leary, P.N., 1991. Stepwise mass extinctions: the case for the Late Cenomanian event. Terra Nova 3, 142–147.

Irwin, H., Curtis, C., Coleman, M., 1977. Isotopic evidence for source of diagenetic carbonates formed during burial of organic-rich sediments. Nature 269, 209–213.

Jablonski, D., 1981. Extinctions: a paleontological perspective. Science 253, 754–757.

Jarvis, I., Carson, G.A., Cooper, M.K.E., Hart, M.B., Leary, P.N., Tocher, B.A., Horne, D., Rosenfeld, A., 1988. Microfossil assemblages and the Cenomanian-Turonian (late Cretaceous) oceanic anoxic event. Cretaceous Research 9, 3–103.

Jenkyns, H.C., Gale, A.S., Corfield, R.M., 1994. Carbon- and oxygen-isotope stratigraphy of the English Chalk and Italian Scaglia and its palaeoclimatic significance. Geological Magazine 131, 1–34.

Johnson, C.C., Barron, E.J., Kauffman, E.G., Arthur, M.A., Fawcett, P.J., Yasuda, M.K., 1996. Middle Cretaceous reef collapse linked to ocean heat transport. Geology 24, 376–380.

Jones, C.E., Jenkyns, H.C., 2001. Seawater strontium isotopes, oceanic anoxic events and seafloor hydrothermal activity in the Jurassic and Cretaceous. American Journal Science 301, 112–149.

Keller, G., 2003. Biotic effects of impacts and volcanism. Earth and Planetary Science Letters 215, 249–264.

Keller, G., Pardo, A., 2004a. Age and paleoenvironment of the Cenomanian-Turonian global stratotype section and point at Pueblo, Colorado. Marine Micropaleontology 51, 95–128.

Keller, G., Pardo, A., 2004b. Disaster opportunists Guembelitrinidae: index for environmental catastrophes. Marine Micropaleontology 53, 83–116.

Keller, G., Han, Q., Adatte, T., Burns, S., 2001. Paleoenvironment of the Cenomanian-Turonian transition at Eastbourne, England. Cretaceous Research 22, 391–422.

Keller, G., Berner, Z., Adatte, T., Stueben, D., 2004. Cenomanian-Turonian $\delta^{13}C$ and $\delta^{18}O$, sea level and salinity variations at Pueblo, Colorado. Palaeogeography, Palaeoclimatology, Palaeoecology 211, 19–43.

Kennedy, W.J., Cobban, W.A., 1991. Stratigraphy and interregional correlation of the Cenomanian-Turonian transition in the Western Interior of the United States near Pueblo, Colorado, a potential boundary stratotype for the base of the Turonian stage. Newsletter of Stratigraphy 24, 1–33.

Kennedy, W.J., Walaszezyk, I., Cobban, W.A., 2000. Pueblo, Colorado, USA, candidate Global Boundary Stratotype Section and Point for the base of the Turonian Stage of the Cretaceous and for the base of the middle Turonian Substage, with a revision of the Inoceramidae (Bivalvia). Acta Geologica Polonica 50, 295–334.

Kolonic, S., Wagner, T., Forster, A., Sinningh Damsté, J.S., Walsworth-Bell, B., Erba, E., Turgeon, S., Brumsack, H.J., Chellai, E.H., Tsikos, H., Kuhnt, W., Kuypers, M.M.M., 2005. Black shale deposition on the northwest African shelf during the Cenomanian-Turonian oceanic anoxic event: climate coupling and global organic carbon burial. Paleoceanography 20, 1006. doi:10.1029/2003PA000950.

Koutsoukos, E.A.M., 1996. Phenotypic experiments into new pelagic niches in early Danian planktonic foraminifera: aftermath of the K/T boundary event. In: Hart, M.B. (Ed.), Biotic Recovery from Mass Extinction Events. Geological Society, Special Publication, vol. 102, pp. 319–335.

Koutsoukos, E.A.M., Leary, P.N., Hart, M.B., 1990. Latest Cenomanian-earliest Turonian low-oxygen tolerant benthonic foraminifera: a case study from the Sergipe Basin (N.E. Brazil) and the western Anglo-Paris Basin (Southern England). Palaeogeography, Palaeoclimatology, Palaeoecology 77, 145–177.

Kübler, B., 1987. Cristallinite de l'illite, méthodes normalisées de préparations, méthodes normalisées de mésures. In: Série ADX, vol. 1. Cahiers Institute Géologie, Neuchâtel, Suisse, 13 pp.

Kuhnt, W., Nederbragt, A., Leine, L., 1997. Cyclicity of Cenomanian-Turonian organic-rich sediments in the Tarfay Atlantic Coastal Basin (Morocco). Cretaceous Research 18, 587–601.

Kuhnt, W., Chellai, E.H., Holbourn, A., Luderer, F., Thurow, J., Wagner, T., El Albani, A., Beckmann, B., Hervin, J.-P., Kawamura, H., Kolonic, S., Nederbragt, A., Street, C., Ravilious, K., 2001. Morocco Basin's sedimentary record may provide correlations for Cretaceous paleooceanographic events worldwide. EOS, Transactions American Geophysical Union 82, 361–364.

Kuhnt, W., Luderer, F., Nederbragt, S., Thurow, J., Wagner, T., 2004. Orbital scale record of the late Cenomanian-Turonian Oceanic Anoxic Event (OAE2) in the Tarfaya Basin (Morocco). International Journal of Earth Sciences 94, 147–159, doi:10.1007/s00531-004-0440-5.

Kuypers, M.M.M., Pancost, R., Sinninghe Damsté, J.S., 1999. A large and abrupt fall in atmospheric CO_2 concentration during Cretaceous times. Nature 399, 342–345.

Lamolda, M.A., Gorostidi, A., Paul, C.R.C., 1994. Quantitative estimates of calcareous nannofossil changes across the Plenus Marls (latest Cenomanian), Dover, England; implication for the generation of the Cenomanian-Turonian boundary event. Cretaceous Research 15, 143–164.

Larson, R.L., Erba, E., 1999. Onset of mid-Cretaceous greenhouse in the Barremian-Aptian: igneous events and biological, sedimentary, and geochemical responses. Paleoceanography 14, 663–678.

Leckie, R.M., 1985. Foraminifera of the Cenomanian-Turonian boundary interval, Greenhorn Formation, Rock Canyon Anticline, Pueblo, Colorado. In: Pratt, L.M., Kauffman, E.G., Zelt, F.B. (Eds.), Fine-grained Deposits and Biofacies of the Cretaceous Western Interior Seaway: Evidence of Cyclic Sedimentary Processes. Society of Economic Paleontologists and Mineralogists Field Trip Guidebook, vol. 4, pp. 139–149.

Leckie, R.M., Yuretich, R.F., West, L.O.L., Finkelstein, D., Schmidt, M., 1998. Paleoceanography of the southwestern Interior Sea during the time of the Cenomanian-Turonian boundary (Late Cretaceous). In: Dean, W.E., Arthur, M.A. (Eds.), Concepts in Sedimentology and Paleontology. Society of Economic Paleontologists and Mineralogists, vol. 6, pp. 101–126.

Leckie, R.M., Bralower, T.J., Cashman, R., 2002. Oceanic anoxic events and plankton evolution: biotic response to tectonic forcing during the mid-Cretaceous. Paleoceanography 17, 1041. doi:10.1029/2001PA000623.

Leine, L., 1986. Geology of the Tarfaya oil shale deposit, Morocco. Geologie en Mijnbouw 65, 57–74.

Luciani, V., Cobianchi, M., 1999. The Bonarelli level and other black shales in the Cenomanian-Turonian of the northeastern Dolomites (Italy): calcareous nannofossil and foraminiferal data. Cretaceous Research 20, 135–167.

Luderer, F., Kuhnt, W., 1997. A high resolution record of the Rotalipora extinction in Laminated organic carbon-rich limestones of the Tarfaya Atlantic coastal Basin (Morocco). Annales de la Société Géologique du Nord (2ème série) 5, 199–205.

Meyers, S.R., Sageman, B.B., Hinnov, L.A., 2001. Integrated quantitative stratigraphy of the Cenomanian-Turonian Bridge Creek Limestone Member using evolutive harmonic analysis and stratigraphic modelling. Journal of Sedimentary Research 71, 627–644.

Meyers, S.R., Sageman, B.B., Lyons, T.W., 2005. Organic burial rate and the molybdenum proxy: theoretical framework and application to Cenomanian-Turonian oceanic anoxic event 2. Paleoceanography 20, 2002. 627–643.

Mitchell, S.F., Ball, J.D., Crowley, S.F., Marshall, J.D., Paul, C.R.C., Veltkamp, C.J., Samir, A., 1997. Isotope data from Cretaceous chalks and foraminiferal environmental or diagenetic signals? Geology 25, 691–694.

Mort, H.P., Adatte, T., Föllmi, K., Keller, G., Steinmann, P., Matera, V., Berner, Z., Stueben, D., 2007. Phosphorus and the roles of productivity and nutrient cycling during oceanic anoxic event 2. Geology 35, 483–486.

Mozley, P.S., Burns, S.J., 1993. Oxygen and carbon isotopic composition of marine carbonate concretions; an overview. Journal of Sedimentary Petrology 63, 73–83.

Nederbragt, A., Fiorentino, A., 1999. Stratigraphy and paleoceanography of the Cenomanian-Turonian boundary event in Oued Mellegue, northwestern Tunisia. Cretaceous Research 20, 47–62.

Norris, R.D., Bice, K.L., Magno, E.A., Wilson, P., 2002. Jiggling the tropical thermostat in the Cretaceous hothouse. Geology 30, 299–302.

Obradovich, J., 1993. A Cretaceous time scale. Geological Association of Canada Special Paper 39, 379–396.

Pardo, A., Keller, G. Biotic effects of environmental catastrophes at the end of the Cretaceous: *Guembelitria* and *Heterohelix* blooms. Cretaceous Research, in this issue.

Paul, C.R.C., Lamolda, M.A., Mitchell, S.F., Vaziri, M.R., Gorostidi, A., Marshall, J.D., 1999. The Cenomanian-Turonian boundary at Eastbourne (Sussex, UK): a proposed European reference section. Palaeogeography, Palaeoclimatology, Palaeoecology 150, 83–121.

Price, G.D., Selwood, B.W., Corfield, R.M., Clarke, L., Cartlidge, J.E., 1998. Isotopic evidence for paleotemperatures and depth stratification of Middle Cretaceous planktonic foraminifera from the Pacific Ocean. Geological Magazine 135, 183–191.

Raiswell, R., Fisher, Q.J., 2004. Rates of carbonate cementation associated with sulphate reduction in DSDP/ODP sediments: implications for the formation of concretions. Chemical Geology 211, 71–85.

Raup, D.M., Sepkoski, J.J., 1982. Periodicity of extinctions in the geological past. Proceedings of the National Academy of Sciences, U S A 81, 801–805.

Robaszynski, F., Caron, M., 1979. Atlas de foraminifères planctoniques du Crétacé moyen (Mer Boreale et Tethys), première partie. Cahiers de Micropaléontologie 1, 185.

Sageman, B.B., Rich, J., Arthur, M.A., Dean, W.E., Savrda, C.E., Bralower, T.J., 1998. Multiple Milankovitch cycles in the Bridge Creek Limestone (Cenomanian-Turonian), Western Interior Basin. In: Dean, W.E., Arthur, M.A. (Eds.), Concepts in Sedimentology and Paleontology. Society of Economic Paleontologists and Mineralogists, vol. 6, pp. 153–171.

Sageman, B.B., Meyers, S.R., Arthur, M.A., 2006. Orbital time scale and new C-isotope record for Cenomanian-Turonian boundary stratotype. Geology 34, 125–128.

Sass, E., Bein, A., Almogi-Labin, A., 1991. Oxygen-isotope composition of diagenetic calcite in organic-rich rocks: evidence for ^{18}O depletion in marine anaerobic pore water. Geology 19, 839–842.

Schlanger, S.O., Arthur, M.A., Jenkyns, H.C., Scholle, P.A., 1987. The Cenomanian-Turonian oceanic anoxic event. I. Stratigraphy and distribution of organic carbon-rich beds and the marine $\delta^{13}C$ excursion. In: Brooks, J., Fleet, A.J. (Eds.), Marine Petroleum Source Rocks. Geological Society, Special Publication, vol. 26, pp. 371–399.

Schrag, D.P., DePaolo, D.J., Richter, F.M., 1995. Reconstructing past sea surface temperatures: correcting for diagenesis of bulk marine carbon. Geochimica et Cosmochimica Acta 59, 2265–2278.

Shaw, A.B., 1964. Time in Stratigraphy. McGraw-Hill, New York, 365 pp.

Sepkoski, J.J., 1989. Periodicity in extinction and the problem of catastrophism in the history of life. Journal of the Geological Society, London 146, 7–19.

Tantawy, A.A. Calcareous nannofossil biostratigraphy and paleoecology of the Cenomanian – Turonian transition at Tazra, Tarfaya Basin, southern Morocco. Cretaceous Research, in this issue.

Tsikos, H., Jenkyns, H.C., Walsworth-Bell, B., Petrizzo, M.R., Forster, A., Kolonic, S., Erba, E., Premoli-Silva, I., Baas, M., Wagner, T., Sinninghe Damsté, J.S., 2004. Carbon isotope stratigraphy recorded by the Cenomanian-Turonian oceanic anoxic event: correlation and implications based on three key localities. Journal of the Geological Society, London 161, 711–719.

Ulicny, D., Hladiková, J., Hradecká, L., 1997. Record of sea-level changes, oxygen depletion and the $\delta^{13}C$ anomaly across the Cenomanian-Turonian boundary, Bohemian Cretaceous Basin. Cretaceous Research 14, 211–234.

Wagner, T., Sinninghe Damsté, J.S., Hofmann, P., Beckmann, B., 2004. Euxinia and primary production in late Cretaceous eastern equatorial Atlantic surface waters fostered orbitally driven formation of marine black shales. Paleoceanography 19, 3009, doi:10.1029/2003PA000898.

Wilson, P.A., Jenkyns, H.C., Elderfield, H., Larson, R.L., 1998. The paradox of drowned carbonate platforms and the origin of Cretaceous Pacific guyots. Nature 392, 889–894.

Appendix

Table 1
Relative species abundances of planktic foraminifera during the upper Cenomanian oceanic anoxic event 2 (OAE2) at Tazra, Tarfaya Basin, southern Morocco

Biozones	*R. cushmani*															*W. archeocretacea*					
Subzones	*A. multiloculata*															G.ben.		*Heterohelix*			
Sample	1	2	3	4	5	6	7	8	9	10	11	12	13	14	15	16	17	18	19	20	21
Depth (m)	0	0.2	0.4	0.6	0.8	1	1.2	1.4	1.6	1.8	2	2.2	2.4	2.6	2.8	3	3.2	3.4	3.6	3.8	4
Anaticella multiloculata	x	x	x	x	x	x			x	x	x	x		x	x	1	x	x			
Dicarinella algeriana													x	x	2	x	x	x			
D. hagni														x	x			x			
D. imbricata						x?							3	x	x	x		3			
Globigerinelloides bentonensis	3	x	2	x	8	6	4					x	1	x	1	1	x				
G. ultramicra	x	x	3	1	2	x	4	1	3	3	3	2	7	3	4	4			1		
Gümbelitria cenomana			2			x	1		3	6	9	7	25	5	1	2	x	x			x
Hedbergella delrioensis	1	x			1	1	3	4	x	x	x	x	x	1	1	2	x	x			x
H. planispira	5	52	53	35	46	44	34	49	42	27	49	41	34	46	35	40	16	82	13	6	31
H. simplex	4	4	5	6	5	7	5	1	x	x	3	9	12	6	14	6	x	3			x
Heterohelix moremani	81	39	12	32	17	28	16	39	36.2	48.3	33	27	5	27	17	17	82	7*	75	89	68
H. reussi	1	1	6	6	2	2										2	2	1			
Praeglobotruncana aumalensis			1	x	x	x	x	x	x	x		x	x	x	1	x		x			
P. gibba					x	x		x	x	x		x		x	1			x			x
P. inornata	x																				
P. helvetica																					
P. praehelvetica									x		x	x		x	x	x					
P. stephani				x	x		x	x			x		x			4	x	x			
Rotalipora cushmani	x	x	x	x		x	x	x	x	x	x	x	x	x	x						
R. deekei	x	x	x	x	x					x	x	x	x	x							
R. greenhornensis	x		x	x	x	x															
Shakoina				x										x	1	x					
Whiteinella aprica	x		2	5	3	x	4	x	2	x	1	x	x	1	1	4	x	x		1	x
W. archaeocretacea	3	3	7	9	8	8	19.6	x	10	9	x	8	6	10	9	7	x	3	7	2	x
W. baltica	1	x	2	2	2	1	8	2	3	6	x	3	x	x	3	6	x	x	4	2	
W. brittonensis	x	x	x	1	x	1	x	x	x	x	1	x	x	x	2	1	x				
W. paradubia	x	x	1	x	x	x	x	x	x	x	x	1		x	2	x	x				
Juvenile specimens no ID			2	3	4	2		4					4		1	2					
Total specimens counted	370	242	283	353	363	331	194	162	157	145	181	352	183	333	371	285	367	331	102	158	434
Benthic Foraminifera	0	10	0	0	0	0	17	42	28	70	258	72	366	111	70	35	0	38	9	10	0
Preservation	G	G	G	G	G	G	P	P	P	P	G	G	G	G	G	G	G	P	L'st	L'st	G

(*continued on next page*)

Table 1 (*continued*)

Biozones	*W. archeocretacea*														*P. helvetica*					
Subzones	*Heterohelix*																			
Sample	22	23	24	25	26	27	28	29	30	31	32	33	34	35	36	37	38	39	40	41
Depth (m)	4.2	4.4	4.6	4.8	5	5.2	5.4	5.6	5.8	6	6.2	6.4	6.6	6.8	7	7.2	7.4	7.6	7.8	8
Anaticella multiloculata									x	x			x	x	0.4	x			x	x
Dicarinella algeriana							1.3	0.5	0.7							x			0.4	x
D. hagni											x								x	x
D. imbricata											x							x		
Globigerinelloides bentonensis																		8		
G. ultramicra	2.7									0.8			3.4							0.9
Gümbelitria cenomana								4.2												
Hedbergella delrioensis													0.7							
H. planispira	15.3	31	22	6	x	0.7	8.5	3.7	12.3	7.3	16.6		15.3	13	31.6	13.4	4	7	5	16
H. simplex	3		x							0.4						0.3		1		
Heterohelix moremani	77.2	69	78	94	100	99	89.4	91.6	83.8	88.5	82.4		80	87	67.5	85.8	10	6	90.4	78.7
H. reussi							0.8			1.2										
Marginotruncana marianosi																		x		
Praeglobotruncana aumalensis	x								x	x	x		x		x	0.3	x	2	x	x
P. gibba											x		x		x	x	x	x		
P. inornata																				
P. helvetica															x	x	x		x	x
P. praehelvetica									x		x				x	x	x		x	x
P. stephani																				
Rotalipora cushmani																				
R. deekei																				
R. greenhornensis																				
Shakoina																				
Whiteinella aprica			x						0.7	x	0.3		x		x	0.3	x		x	x
W. archaeocretacea	1.2								2.2		0.7				0.4		x	5	4.2	4.4
W. baltica	0.3								0.4	2.3			0.7		0.4		x	x		
W. brittonensis									x	x							x	x		
W. paradubia																				
Juvenile specimens no ID																				
Total specimens counted	333	216	385	269	269	269	236	215	277	261	301		150	270	237	373			260	225
Benthic Foraminifera	0	0	0	0	0	0	0	0	0	8	0		0	0	0	0	0	0	0	0
Preservation	G	G	G	G	G	G	G	G	M	M	M		P	M	G	G	P	P	G	P

G = good, M = medium, P = poor.

* poor preservation, many broken biserials and isolated chambers, therefore not reliable census.

Table 2
Bulk rock stable isotopes (oxygen and carbon) across the late Cenomanian oceanic anoxic event 2 (OAE2) at Tazra, Tarfaya Basin, southern Morocco

Samples	$d^{13}C$	$d^{18}O$
	VPDB	VPDB
1	0.05	−3.69
1, duplicate	0.05	−3.71
2	0.08	-4.33
3	−0.83	−3.55
4	0.45	−4.59
5	0.67	−4.48
6	0.51	−4.44
7	1.88	−3.37
8	1.87	−3.63
9	1.96	−3.55
10	2.63	−3.53
11	2.93	−3.22
12	2.54	−4.06
13	2.27	−3.52
14	1.98	−4.35
14, duplicate	2.04	−4.19
15	1.45	−4.62
16	0.89	−4.70
17	0.95	−3.79
18	1.22	−4.30
19	1.71	−4.08
20	1.39	−4.25
21	1.54	−3.87
22	0.26	−4.05
23	2.09	−4.29
24	1.05	−4.27
24,duplicate	1.47	−4.28
25	1.04	−4.75
26	2.57	−4.39
27	−0.88	−5.30
28	1.27	−4.75
29	1.49	−4.84
30	0.32	−2.98
31	1.15	−3.80
32	1.33	−4.05
33	0.41	−3.96
34	1.24	−4.09
35	0.95	−4.04
36	1.54	−4.12
37	0.60	−4.60
38	1.28	−4.43
39	0.32	−7.40
40	0.76	−4.34
41	0.12	−4.66
42	−1.36	−3.80